

Optimizing Minimum Vertex Cover Solving via a GCN-assisted Heuristic Algorithm

Enqiang Zhu^a, Qiqi Bao^a, Yu Zhang^b, Chanjuan Liu^{*c}

^a*Institute of Computing Science and Technology, Guangzhou University, Guangzhou, 510006, China*

^b*School of Computer Science, Peking University, Beijing, 100091, China*

^c*School of Computer Science and Technology, Dalian University of Technology, Dalian, 116024, China*

Abstract

The problem of finding a minimum vertex cover (MVC) in a graph is a well-known \mathcal{NP} -hard problem with significant practical applications in optimization and scheduling. Its complexity, combined with the increasing scale of problems, underscores the need for efficient and effective algorithms. However, existing heuristic algorithms for MVC often rely on simplistic initialization strategies and overlook the impact of edge attributes and neighborhood information on vertex selection. In this paper, we introduce GCNIVC, a novel heuristic search algorithm designed to address the limitations of existing methods for solving MVC problems in large-scale graphs. Our approach features two main innovations. First, it utilizes a Graph Convolutional Network (GCN) to capture the global structure of graphs, which enables the generation of high-quality initial solutions that enhance the efficiency of the subsequent search process. Second, GCNIVC introduces a new heuristic that employs three containers and the concept of double-covered edges (dc-edges), improving search efficiency and providing greater flexibility for adding and removing operations based on edge attributes. Through extensive experiments on benchmark datasets, we demonstrate that GCNIVC outperforms state-of-the-art MVC algorithms in terms of both accuracy and efficiency. Our results highlight the effectiveness of GCNIVC's GCN-assisted initialization and its edge-informed search strategy. This study not only advances the understanding of MVC problem-solving but also contributes a new tool for addressing large-scale graph optimization challenges.

Keywords: Minimum vertex cover (MVC); Heuristic search; Deep learning; Optimization; Graph convolution network (GCN); Large-scale problem.

1. Introduction

Given an undirected graph $G = (V, E)$, the minimum vertex cover (MVC) problem is tasked with identifying the smallest subset C of vertices such that each edge $e \in E$ has at least one of its endpoints included in C .

Recognized as an \mathcal{NP} -hard problem [1, 2], MVC is not only theoretically significant but also crucial for a multitude of real-world applications in optimization and scheduling [3]. Key applications include identifying influential users to maximize social network impact, ensuring router coverage and sensor deployment in communication networks, and analyzing protein interactions to optimize gene regulation in bioinformatics. For example, in social networks, the MVC problem can help identify key users who can effectively expand outreach or communication. It also plays a role in optimizing facility locations, maintaining power grids, and allocating

resources efficiently by covering critical relationships with the minimal number of nodes.

1.1. Background

As technology progresses, the scale of MVC problems, such as influence propagation, router coverage, and sensor deployment, has grown significantly. Traditional algorithms struggle with the computational efficiency and solution quality required for these large-scale instances. These algorithms are generally categorized into two types: exact algorithms and approximation algorithms.

Among the exact methods, branch-and-bound algorithms are a key technique to reduce the base of exponential running time [4, 5]. The core idea is to systematically explore the solution space by dividing it into smaller subproblems and using bounds to discard subproblems that cannot yield better solutions than the cur-

rent best. However, these exact algorithms cannot eliminate the exponential time complexity, making them impractical for large-scale MVC instances.

Approximation algorithms have been developed to provide near-optimal solutions effectively. Greedy algorithms, known for their simplicity, are often used to approximate solutions for \mathcal{NP} -hard problems, including the connected dominating set, weighted vertex cover, independent set problems, and flow shop scheduling problem [6, 7, 8, 9]. The greedy approach involves making a series of locally optimal choices, such as selecting the vertex with the highest degree at each step to cover the most edges. While greedy algorithms can generate feasible solutions quickly, the quality of these solutions often fails to meet real-world application demands.

Heuristic methods are often employed to solve large-scale \mathcal{NP} -hard problems, as they can provide near-optimal solutions within a reasonable time limit [10, 11, 12, 3, 13, 14]. The heuristic approach for MVC typically involves two main steps: initialization and search. The initialization process aims to produce a relatively high-quality solution quickly, which is then iteratively refined during the search stage through operations like node exchange. Existing algorithms often rely on random initialization or simple strategies, such as selecting high-degree vertices, to construct the initial solution. Recent studies highlight the significant impact of the initialization mechanism on heuristic algorithm performance [15]. Therefore, improving the initialization mechanism for heuristic algorithms in MVC is crucial. Moreover, during the search phase, existing algorithms focus on identifying higher-quality vertices but overlook the impact of different edges and neighboring information on vertices, which is detrimental to efficient space search.

1.2. Our Contributions

In this paper, we introduce GCNIVC, a novel heuristic search algorithm designed for MVC on large-scale graphs. GCNIVC leverages a graph convolutional network (GCN) to capture the holistic structure of graphs and generate a high-quality initial solution. By integrating edge search and container optimization strategies, GCNIVC enhances heuristic search performance.

Our contributions are summarized as follows:

(1) Based on the GCN framework, GCNIVC uses the probabilities of vertices generated by the neural network to produce a high-quality initial solution. This approach offers a new perspective for addressing the MVC problem by harnessing the learning capabilities of neural networks to understand the relationships between a ver-

tex’s neighbors and the overall structure of the graph, thereby enhancing the quality of the initial solution.

(2) We introduce a new heuristic for MVC that incorporates three containers and proposes the concept of double-covered edges (dc-edges), which integrates three types of edges and utilizing their structural features to further improve solution quality and enhance search efficiency.

We have conducted experiments on multiple benchmark datasets to verify the performance of the proposed algorithm. The results show that GCNIVC demonstrates superior performance in accuracy and efficiency compared to state-of-the-art MVC algorithms.

1.3. Organization of This Paper

The rest of the paper is structured as follows: Section 2 offers an overview of related work on heuristic search algorithms for the Minimum Vertex Cover (MVC) problem. Section 3 presents foundational knowledge, including key definitions in graph theory, the heuristic framework, and an introduction to graph neural networks. In Section 4, we delve into the main components of our algorithm, which has been developed through a thorough research process. Our experimental results are discussed in Section 5. Finally, Section 6 concludes the paper with potential directions for future work.

2. Related Work

Heuristic algorithms for the Minimum Vertex Cover (MVC) problem have been extensively studied. For example, EdgeGreedyVC [16] improves a partial solution by repeatedly adding the endpoint of an uncovered edge that has the maximum degree and then removing any redundant vertices. Although EdgeGreedyVC enhances the quality of the solution by reducing the size of the vertex cover without sacrificing coverage, it only takes into account the local structure of the graphs.

Cai et al. [17] introduced a two-stage exchange strategy and an edge weighting mechanism to develop a heuristic search algorithm for the Minimum Vertex Cover (MVC) problem, named NuMVC. This method aimed to resolve the inefficiencies caused by the simultaneous selection of vertices in earlier studies [18, 19]. However, it encountered significant challenges when addressing large-scale instances.

In 2015, Cai et al. [16] proposed the Best from Multiple Selections (BMS) heuristic, which involves randomly sampling vertices from a candidate set and removing the one with the minimum loss value. This approach contributed to the development of FastVC, an algorithm specifically designed to efficiently handle large

instances of the Minimum Vertex Cover (MVC) problem.

Ma et al. [20] further refined this approach by integrating a noisy selection strategy into BMS, resulting in the NoiseVC algorithm. They also presented the WalkBMS algorithm, which probabilistically chooses between BMS and a random walk for vertex selection, addressing local optima issues in FastVC [16]. Subsequently, Cai et al. [21] proposed an improved version of FastVC, named FastVC2+p, which integrates additional processing techniques and enhances initial solution construction methods. More recently, Luo et al. [22] introduced MetaVC, a highly parametric heuristic framework that utilizes various effective heuristic search techniques. This framework includes an automatic algorithm configurator aimed at optimizing performance based on the parameters of each instance.

Later, Quan et al. [23] proposed EABMS, a new edge weighting method based on edge age, which led to the development of EAVC and its variant EAVC2+p. Both demonstrated superior performance on large graphs compared to previous methods, including FastVC, MetaVC, and their variants. Recently, Zhang et al. [24] introduced a novel edge weighting method based on vertex age, known as TIVC, and developed the TIVC algorithm. This algorithm demonstrated significant superiority over other methods in graph processing tasks. The introduction of the TIVC algorithm marks a pivotal advancement in understanding the role of vertex age in the MVC problem.

Overall, FastVC, EAVC, TIVC, and their variants represent the state-of-the-art heuristic search algorithms for MVC, especially for handling large instances. Their effectiveness has been validated through comparisons with baseline algorithms. However, despite these advancements, several critical limitations persist in practical applications. These limitations include inadequate consideration of initial solutions and a failure to account for the impact of different edges during the iterative improvement process. To tackle these challenges, this study incorporates the GCN framework to enhance the quality of initial solutions and improve overall solution quality by influencing vertex selection using various types of edges.

3. Preliminaries

The following section presents foundational information. Specifically, Section 3.1 presents pertinent notations and terminologies, Section 3.2 succinctly outlines the heuristic search method, and Section 3.3 introduces the graph neural network.

3.1. Notations and Terminologies

Let's consider an undirected graph $G = (V, E)$ with a vertex set V and an edge set E . For an edge $e = (u, v)$, the vertices u and v are referred to as the *endpoints* of e . If two vertices are the endpoints of an edge, they are considered *adjacent*, and one is called a *neighbor* of the other. An edge is *incident* with its endpoints, and vice versa. The set containing all neighbors of a vertex $v \in V$ is denoted by $N(v)$ and is called the *neighborhood* of v . The *closed neighborhood* of v , denoted by $N[v]$, is defined as $N[v] = N(v) \cup \{v\}$. The *degree* of v , denoted by $d(v)$, is the number of edges incident with v . For a vertex set $S \subseteq V$, let $N[S] = \bigcup_{v \in S} N[v]$ and $N(S) = N[S] \setminus S$.

In a graph $G = (V, E)$, a set of vertices $S \subseteq V$ *covers* an edge $e \in E$ if at least one of the endpoints of e belongs to S . If all edges of G are covered by S , then S is called a *vertex cover* (VC) of G . A vertex cover with the smallest cardinality is called a *minimum vertex cover* (MVC) of G . Notably, a graph $G = (V, E)$ may have more than one MVC. We use $E_u(S) \subseteq E$ to denote the set of edges uncovered by S and $E_c(S) \subseteq E$ to denote the set of edges covered by S . The MVC problem involves finding an MVC for a given graph.

3.2. Heuristic Search

In the context of the MVC problem, we use C to denote a candidate (or partial) solution. The general approach for heuristic search in MVC involves initially constructing a VC and then iteratively improving the solution to a smaller one by swapping vertices. The LS algorithms typically utilize $\text{gain}(v)$ and $\text{loss}(v)$ to assess the importance of a vertex v . Here, $\text{gain}(v)$ represents the number of edges uncovered by C but covered by $C \cup \{v\}$, while $\text{loss}(v)$ is the number of edges covered by C but uncovered by $C \setminus \{v\}$. The “age” of a vertex v , denoted by $\text{age}(v)$, refers to the number of steps since it was last removed from C . Age values are often used to break ties when multiple vertices have the same *gain* or *loss* value. Additionally, the “age” of an edge e , denoted by $\text{age}(e)$, represents the number of steps since it was last uncovered by C . This criterion is commonly used for selecting edges [23, 24].

3.3. Graph Neural Network

In recent years, graph convolutional networks (GCN) have emerged as a popular framework for directly learning from graph-structured data using deep learning. GCNs aim to learn how to transform node features by considering the feature values and the graph structure. They learn node embeddings through information

propagation between nodes and their neighbors, making them widely applicable to tasks such as node classification, graph embedding, and graph clustering [25, 26]. The core idea of GCNs is to extend the convolution operation to irregular graph structures, thereby aggregating features based on the adjacency relationships within the graph. GCNs define the neighborhood relationships between nodes using the graph’s adjacency matrix, aggregating the features of each node along with those of its neighboring nodes. Consequently, the representation of a node depends not only on its features but also on the feature information of its neighbors.

The model essentially functions as a message-passing mechanism, where the convolution operation at each layer can be interpreted as each node receiving and aggregating information from its neighboring nodes. This mechanism allows GCNs to progressively broaden the influence of each node, thereby integrating structural information from a broader range within the graph. Formally, it can be described as follows:

$$H^{(\ell+1)} = \sigma\left(\tilde{D}^{-\frac{1}{2}}\tilde{A}\tilde{D}^{-\frac{1}{2}}H^{(\ell)}W^{(\ell)}\right).$$

Here are some details about the terms used in this equation:

- The matrix $H^{(\ell)} \in \mathbb{R}^{N \times D^{(\ell)}}$ represents the node feature matrix at layer ℓ , where $\ell \geq 0$. In this context, N denotes the number of nodes in the graph, and $D^{(\ell)}$ represents the feature dimension at layer ℓ . The initial node feature matrix $H^{(0)}$ corresponds to the input node feature matrix.
- The normalized adjacency matrix, denoted as \tilde{A} , is obtained using the formula $\tilde{A} = \hat{D}^{-\frac{1}{2}}\hat{A}\hat{D}^{-\frac{1}{2}}$. This method ensures numerical stability and balanced feature aggregation. In this context, $\hat{A} = A + I$ is derived from adding the original adjacency matrix A to the identity matrix I . The degree matrix \hat{D} normalizes the adjacency matrix.
- The matrix $W^{(\ell)} \in \mathbb{R}^{D^{(\ell)} \times D^{(\ell+1)}}$ denotes the trainable weight matrix at layer ℓ .
- The function $\sigma(\cdot)$ serves as a non-linear activation function, such as ReLU, and is responsible for introducing non-linearity into the model.

4. Main Algorithm

In this section, we introduce our algorithm GCNIVC. We first discuss two main components of GCNIVC: GCNConstructVC, which is responsible for constructing the initial solution, and ContainerRemoveVertex,

which optimizes the process of removing vertices from a current solution. After that, we will provide a detailed description of the algorithm.

4.1. GCNConstructVC

In the initial stage of LS algorithms for MVC, a small-scale initial VC (the initial solution) can effectively minimize unnecessary computation during the subsequent search process, thereby accelerating the convergence towards a high-quality solution. However, it is crucial to balance the quality of the initial solution and the time required to construct it. Overemphasizing either aspect could render the algorithm inefficient in practical applications. Therefore, it is necessary to consider not only the local structure of a graph but also its global structure. To address this, we introduce the GCN to the initialization process and develop an algorithm GCNConstructVC to effectively generate a high-quality initial solution.

A GCN takes an $n \times d$ node feature matrix and an $n \times n$ adjacency matrix as inputs and produces a $n \times k$ feature matrix as output, where n represents the number of nodes, d denotes the number of input features for each node, and k indicates the number of output features for each node. In our specific task, the input features comprise four components (i.e., $d = 4$): nodes’ weight (set to 1 for all vertices in our experiment), nodes’ degree, graph’s density $\frac{m}{n^2}$ (m denotes the number of edges), and the difference between a node and the mean value of its neighbors $\frac{1}{|N(v)|} \sum_{u \in N(v)} d(u)$. The output consists of the probabilities of nodes belonging to an MVC. A general structure of a GCN is depicted in Figure 1. Small graphs are utilized to train the model, including T1/T2 and UDG instances with a maximum of 250 vertices. The exact algorithm EMVC, proposed by Wang et al. [27] is employed to determine MVCs for these small graphs. Note that only small graphs are utilized for training due to the inefficiency of existing exact MVC algorithms for large-scale graphs.

Algorithm 1 presents the pseudocode of ConstructVC. The algorithm comprises four parts. In the first part, the probability $prob(v)$ of each vertex v belonging to a minimum vertex cover (MVC) is computed using a GCN model (line 2). It’s important to note that this probability alone is insufficient for estimating the importance of vertices, as some vertices may have a high degree but a low probability, and vice versa. To address this, the second part (lines 3-12) introduces a new parameter called $pscore$, a function on the set of vertices.

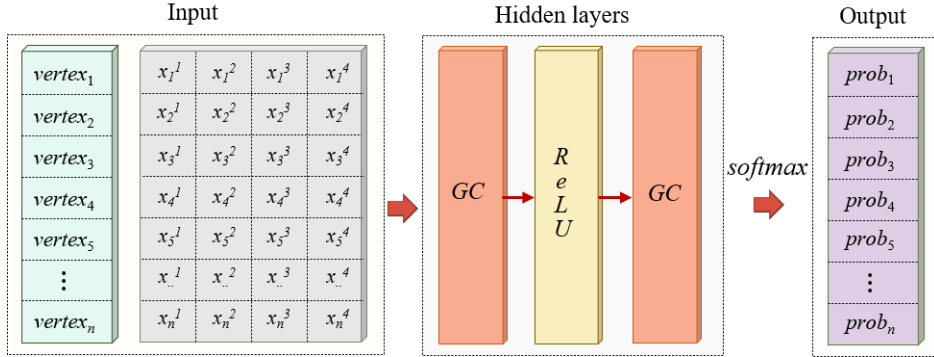


Figure 1: The framework of a GCN for the probabilistic determination of vertices within a minimum vertex cover.

Algorithm 1 GCNConstructVC

Input: graph $G = (V, E)$
Output: A vertex cover C of G

```

1:  $C \leftarrow \emptyset$ ;
2:  $prob \leftarrow$  a function derived from a GCN model that assigns a probability to each vertex (indicating the likelihood of a vertex belonging to an MVC);
3: for each vertex  $v \in V$  do
4:    $pscore(v) \leftarrow d(v)$ ;
5: end for
6: for each edge  $v_1v_2 \in E$  do
7:   if  $prob(v_1) > prob(v_2)$  then
8:      $pscore(v_1) \leftarrow pscore(v_1) + 1$ ;
9:   else if  $prob(v_1) < prob(v_2)$  then
10:     $pscore(v_2) \leftarrow pscore(v_2) + 1$ ;
11:   end if
12: end for
13: for each  $e = v_1v_2 \in E$  do
14:   if  $e$  is uncovered then
15:     if  $pscore(v_1) > pscore(v_2)$  then
16:        $C \leftarrow C \cup \{v_1\}$ ;
17:     else if  $pscore(v_1) < pscore(v_2)$  then
18:        $C \leftarrow C \cup \{v_2\}$ ;
19:     end if
20:   end if
21: end for
22: for each  $v \in C$  do
23:    $loss(v) \leftarrow 0$ ;
24: end for
25: for each  $e \in E$  do
26:   if only one endpoint  $v$  of  $e$  belongs to  $C$  then
27:      $loss(v)++$ ;
28:   end if
29: end for
30: for each  $v \in C$  do
31:   if  $loss(v) = 0$  then
32:      $C = C \setminus \{v\}$ ; update loss of vertices in  $C$ ;
33:   end if
34: end for
35: return  $C$ 

```

This parameter combines the probability and the degree of vertices. Specifically, for each vertex v , $pscore(v)$ is initialized as its degree (lines 3-5). Then, for each edge v_1v_2 , if the probability of v_1 (or v_2) is greater than that of v_2 (or v_1), the value of $pscore(v_1)$ (or $pscore(v_2)$) is increased by one (lines 6-12).

The third part focuses on extending a partial solution C to form a VC based on the $pscore$ (lines 13-21). For each edge v_1v_2 , if $pscore(v_1)$ (or $pscore(v_2)$) is greater than $pscore(v_2)$ (or $pscore(v_1)$), then v_1 (or v_2) is added to C . Finally, the fourth section aims to optimize C by removing redundant vertices using the $loss$ function (lines 22-35). The $loss$ value of each vertex v is initialized to zero (lines 22-24). For each edge e , if C contains exactly one endpoint v of e , then $loss(v)$ is increased by one (lines 25-29). Subsequently, for each vertex $v \in C$, it is removed from C if $loss(v) = 0$ (lines 30-34).

4.2. ContainerRemoveVertex

Vertex exchange is essential for optimizing solutions in an heuristic search algorithm. This process involves removing vertices from a current solution C and adding vertices not in C to C . The quality of the vertices to be removed is crucial for enhancing the algorithm's efficiency. To address this, we introduce a heuristic method called ContainerRemoveVertex (CRV) to identify the vertex in C for the subsequent vertex exchange.

In Algorithm 2, the CRV procedure takes a solution C , three containers $ctner_1$, $ctner_2$, and $ctner_3$ of vertices, an integer num , and a function age associated with vertices as input. It outputs a partial solution of the graph. When any of $ctner_1$, $ctner_2$, or $ctner_3$ is not empty, it randomly selects a vertex v from the union of these containers (lines 1-2). It then iterates through each container num times, choosing a random vertex u each time, and updates v with u if $d(v) \times age(u) < d(u) \times age(v)$ (lines 3-10). Finally, it removes v from C . On the other

hand, if $ctner_1 \cup ctner_2 \cup ctner_3 = \emptyset$, it removes a vertex with the smallest *loss* value from C , resolving ties based on the *age* of the vertex (line 13).

This method provides two primary advantages: A higher likelihood of selecting vertices with lower degrees and the variability in vertex selection due to the random selection mechanism, thereby reducing the risk of prolonged heuristic search cycles under identical conditions.

Algorithm 2 ContainerRemoveVertex (CRV)

Input: A vertex cover C , three containers $ctner_1$, $ctner_2$, and $ctner_3$, and an integer num , a function *age*
Output: A (partial) vertex cover C of G

```

1: if  $(ctner_1 \cup ctner_2 \cup ctner_3) \neq \emptyset$  then
2:    $v \leftarrow$  a random vertex from  $ctner_1 \cup ctner_2 \cup ctner_3$ ;
3:   for each  $ctner \in \{ctner_1, ctner_2, ctner_3\}$  do
4:     for  $i = 0; i < num; i + +$  do
5:        $u \leftarrow$  a random vertex from  $ctner$ ;
6:       if  $d(v) \times age(u) < d(u) \times age(v)$  then
7:          $v \leftarrow u$ ;
8:       end if
9:     end for
10:   end for
11:    $C \leftarrow C \setminus \{v\}$ ;
12: else
13:   Remove the vertex with the minimum loss from  $C$ , resolving ties by the age of vertex;
14: end if
15: return  $C$ 
```

4.3. GCNIVC

Our GCNIVC algorithm takes a graph $G = (V, E)$, a time limit $cutoff$, and an integer num as inputs and produces a VC C^* of G . It begins by generating an initial solution C using GCNConstructVC and initializing various parameters, including three containers $ctnr_1$, $ctnr_2$, $ctnr_3$, and the age of each vertex. Subsequently, it enters a loop to improve the current solution C iteratively. We introduce a new type of edge, called double-covered edge (dc-edge), to streamline the iteration process.

Definition 1: Let C be a partial VC of a graph $G = (V, E)$. An edge $e \in E$ is defined as a *double-covered edge* (dc-edge) if both endpoints belong to C . The *double-covered number* (or *dcnumber* simply) of a vertex v , denoted by $dcnumber(v)$, is the number of dc-edges incident with the vertex.

When removing a vertex from the current solution C , we prioritize those with smaller *dcnumber* values. This is because removing such a vertex may cause only a small number of vertices in its neighborhood to experience an increase in their *loss* values, thus reducing

the number of uncovered edges resulting from removing vertices. Conversely, when adding a vertex to C , we prioritize those with larger *dcnumber* values. This is because adding such a vertex may cause a large number of vertices in its neighborhood to experience a decrease in their *loss* values, thereby reducing the number of vertices with a higher *loss* value in the graph and enhancing the diversity of deleting vertices by BMS strategy in subsequent operations.

Algorithm 3 GCNIVC

Input: A graph $G = (V, E)$, a time limit $cutoff$, an integer num
Output: A vertex cover C^* of G

```

1:  $C \leftarrow$  GCNConstructVC( $G$ )
2:  $ctner_i \leftarrow$  the set of vertices of degree  $i$  in  $G$ , for  $i = 1, 2, 3$ ;
3:  $age(v) \leftarrow 1$ , for each vertex  $v \in V$ ;
4: while elapsed_time  $< cutoff$  do
5:   if  $C$  covers all edges then
6:      $C^* \leftarrow C$ ;
7:      $C \leftarrow$  ContainerRomoveVertex( $C$ ,  $ctner_1$ ,  $ctner_2$ ,  $ctner_3$ ,  $num$ , age);
8:   end if
9:    $u_1 \leftarrow$  a vertex in  $C$  selected by BMS heuristic, breaking ties sequentially by age and dcnumber;
10:   $C \leftarrow C \setminus \{u_1\}$ ;
11:   $u_2 \leftarrow$  a random vertex in  $C$ ;
12:   $C \leftarrow C \setminus \{u_2\}$ ;
13:   $e \leftarrow$  an edge in  $E_u(C)$  selected by BMS heuristic;
14:   $w_1 \leftarrow$  the endpoint of  $e$  with a larger gain value, breaking ties sequentially by age and dcnumber;
15:   $C \leftarrow C \cup \{w_1\}$ ;
16:  if  $E_u(C) \neq \emptyset$  then
17:     $e \leftarrow$  a random edge in  $E_u(C)$ ;
18:     $w_2 \leftarrow$  the endpoint of  $e$  with a larger gain value, breaking ties sequentially by age and dcnumber;
19:     $C \leftarrow C \cup \{w_2\}$ ;
20:  end if
21: end while
22: return  $C^*$ 
```

In each iteration, the algorithm utilizes the (3,2)-swap framework to optimize solutions, consisting of two phases: vertex removal and vertex addition. If C covers all edges in the vertex removal phase, the algorithm updates the best solution C^* with C and removes a vertex from C using the CRV procedure (lines 5-8). Subsequently, two additional vertices are removed from C using the BMS heuristic and a random strategy, respectively, with ties resolved sequentially based on the vertices' *age* and *dcnumber* (lines 9-12). In the vertex addition phase, the algorithm selects an edge from the set of edges not covered by C and adds an endpoint of

the edge with a larger *gain* to C , resolving ties sequentially based on the age and *dnumber* of vertices (lines 13-15). Furthermore, if C still does not cover edges of G , i.e., $E_u(C) \neq \emptyset$, the algorithm randomly selects an edge from $E_u(C)$ and adds an endpoint of the edge with a larger *gain* to C , resolving ties sequentially based on the *age* and *dnumber* of vertices (lines 16-20).

5. Experiments

The performance of the GCNIVC algorithm is evaluated through experiments on various benchmark datasets. In the subsequent section, we describe the benchmark datasets and the experiment setup. We then present the experimental results, which include the sizes of the vertex covers produced by the algorithms under identical conditions, along with an analysis of their convergence times to achieve a final solution. We empirically evaluate the parameters within the GCNIVC algorithm, followed by a comprehensive discussion of the experimental findings.

5.1. Benchmark Datasets

We investigate the MVC problem using multiple benchmark datasets. These datasets include three benchmarks (*UDG* and T_1/T_2) of small graphs for training the GCN model and four benchmarks (*DIMACS 10*, *SNAP*, *NetworkRepository*, *Gset*) of large sparse real-world graphs for testing the algorithms. All instances are treated as undirected, unweighted simple graphs.

*UDG*¹: It contains graphs commonly used to simulate wireless sensor networks or other spatially distributed networks. In these graphs, each vertex represents the center of a unit disk, and edges exist between vertices whose corresponding disks overlap. Unit disk graphs (UDGs) are typically sparse, as each node only connects to nearby nodes, resulting in a relatively low overall degree of connectivity. This dataset comprises 12 families, each containing ten instances of unit disk graphs with 50 to 1000 vertices.

T_1/T_2 ²: This dataset comprises 53 families, each containing ten instances related to graph partitioning and clustering problems in graph theory and network science. The instances in each family have the same size, ranging from 50 to 1000.

*DIMACS 10*³: This dataset provides biologically relevant networks widely used to study graph partitioning

and graph clustering problems [28]. It comprises 130 sparse instances with 1,024 to 23,947,347 vertices.

*SNAP*⁴: It is a comprehensive network analysis platform designed to study and process large-scale networks. It encompasses diverse real-world instances, encompassing social, biological, and technical networks. This dataset comprises 13 instances with 1,005 to 3,774,768 vertices.

*NetworkRepository*⁵: This dataset platform is dedicated to storing and sharing various network datasets commonly utilized in network science, machine learning, data mining, and graph theory. This dataset comprises 127 instances with 39 to 23,947,347 vertices.

*Gset*⁶: The dataset, originating from the University of Iowa, was utilized by Ye et al. [29] to test the dual scaling algorithm. To assess GCNIVC, we collect all instances utilized in the dataset, each comprising between 800 and 7,000 vertices.

5.2. Experiment Setup

All algorithms were implemented in C++ and compiled using gcc 7.1.0 with the '-O3' optimization option. The experiments were conducted on CentOS Linux 7.6.1810, using an Intel(R) Xeon(R) Gold 6254 CPU running at 3.10 GHz, 256 GB memory, and a V100 graphics card. TIVC, FastVC, and EAVC parameter settings are consistent with those reported in the original literature [24, 16, 23]. No data preprocessing techniques were employed during the experiments to ensure a fair comparison with other algorithms. The parameter *num* in the BMS heuristic and *CRV* was set to a random value in the range of 45 to 55, following the authors' suggestion [16], and was ultimately set to 50.

GCNIVC was compared against three state-of-the-art heuristic search algorithms: FastVC [16], EAVC [23], and TIVC [24]. These algorithms are all designed to address the MVC problem for large-scale instances. FastVC integrates a two-stage exchange framework and a BMS heuristic, striking an effective balance between solution accuracy and computational efficiency, particularly for large graphs. EAVC, based on a two-stage framework, employs WalkBMS and EABMS strategies, providing effective guidance in vertex and edge selection phases. TIVC introduces an efficient heuristic search algorithm for MVC, featuring an innovative 3-improvement framework with minor perturbations. This framework allows the algorithm to directly search for

¹<https://github.com/yiyuanwang1988/MDSClassicalBenchmarks>

²<https://github.com/yiyuanwang1988/MDSClassicalBenchmarks>

³<https://www.cc.gatech.edu/dimacs10/downloads.shtml>

⁴<https://snap.stanford.edu/data/>

⁵<https://networkrepository.com>

⁶<git://dollar.biz.uiowa.edu/pub/yyye/Gset/>

solutions of size $k - 2$ after adding a vertex to a feasible solution of size k . Additionally, TIVC introduces a highly efficient edge selection strategy, significantly accelerating the search process. The source codes for FastVC and EAVC are publicly available: FastVC⁷, EAVC⁸.

We executed the FastVC, EAVC, TIVC, and GCNIVC algorithms on each instance ten times, employing random seeds ranging from 1 to 10. Each run was conducted on a dedicated CPU core, with a cutoff time of 1000 seconds. For every instance, we presented the best size (Min.) and the average size (Avg.) of the solutions identified by the algorithms across the ten runs. Additionally, we included the average convergence time (t_Avg.) for each algorithm to determine its final solution on an instance. If an algorithm did not achieve the optimal solution, the average convergence time was recorded as “-”.

5.3. Experimental Result

We analyzed the experimental results from running FastVC, EAVC, TIVC, and GCNIVC across all benchmark datasets. Table 1 highlights the competitive advantages of GCNIVC compared to the other three algorithms across various benchmarks. It presents the number of instances (within each benchmark) where an algorithm performs best and outperforms all other algorithms. As illustrated in Table 1, GCNIVC consistently outperforms the other three algorithms, demonstrating particularly strong performance on the DIMACS10 benchmark.

5.3.1. Comparison of solution quality

The results of the four algorithms FastVC, EAVC, TIVC, and GCNIVC across all benchmark instances are detailed in Tables 2 to 7 (Tables 6 and 7 are in Appendix). The optimal solutions identified by each algorithm are emphasized in bold. Among the 302 benchmark instances, GCNIVC achieved optimal minimum values in 268 cases, followed by TIVC in 212, EAVC in 203, and FastVC in 199 cases. Furthermore, GCNIVC, TIVC, EAVC, and FastVC attained strictly optimal minimum values in 69, 11, nine, and eight instances, respectively. Obviously, GCNIVC exhibits remarkable performance regarding solution quality (Min.). We proceed to discuss the results in more detail.

⁷<http://lcs.ios.ac.cn/caisw/VC.html>

⁸<https://github.com/quancs/EAVC>

| DATASET | GCNIVC | FastVC | TIVC | EAVC |
|--------------------|--------|--------|-------|-------|
| SNAP | 12/1 | 11/0 | 12/1 | 11/0 |
| Gset | 32/0 | 32/0 | 32/0 | 32/0 |
| Network Repository | 123/5 | 116/1 | 120/2 | 116/0 |
| DIMACS10 | 101/63 | 40/8 | 48/8 | 43/8 |

Table 1: Summarizing the number of instances in which an algorithm demonstrates strong performance, where x/y indicates that on x instances, the algorithm achieves the optimal solution, and on y instances, it surpasses all other algorithms.

In the DIMACS10 benchmark, GCNIVC achieved the optimal solutions in 101 out of 130 instances. In contrast, the FastVC, TIVC, and EAVC algorithms secured the best solutions in 40, 48, and 43 cases, respectively. In the SNAP benchmark, GCNIVC continued to lead, attaining the best solutions in 12 out of 13 instances, while FastVC, TIVC, and EAVC each achieved the top solutions in 11 cases. For the Network Repository benchmark, GCNIVC once again excelled, obtaining the best solutions in 124 out of 127 instances. FastVC, TIVC, and EAVC followed closely, with their best solutions achieved in 116, 120, and 117 cases, respectively. Lastly, since the instances in the Gset benchmark are small, all algorithms successfully attained the best solutions across all 32 instances. Moreover, GCNIVC outperformed the other algorithms by producing smaller VCs in 63 instances from DIMACS10, five from Network Repository, and one from SNAP. TIVC found smaller VCs in eight instances from DIMACS10, two from Network Repository, and one from SNAP. EAVC generated smaller VCs in eight instances from DIMACS10, while FastVC found smaller VCs in eight instances from DIMACS10 and one from Network Repository. In addition, among the 302 instances, the GCNIVC, TIVC, EAVC, and FastVC algorithms achieved the smallest average values (Avg.) in 255, 183, 196, and 186 instances, respectively. The above comparisons demonstrate that GCNIVC has a superior performance compared to the other algorithms, highlighting its notable effectiveness across these extensive, sparse real-world benchmarks.

5.3.2. Analysis of convergence speed

We generated convergence curves to analyze how the size of solutions evolves for each algorithm throughout the search process. Generally, heuristic search algorithms exhibit rapid convergence in the early stages, resulting in steep decline curves, particularly in smaller instances. This phenomenon makes it challenging to differentiate between the curves of various algorithms. To address this, we established an upper bound threshold for the MVC in each graph, omitting any segments that surpassed this threshold. This strategy effectively

Table 2: Experimental results on DAMACS10.

| Instance | GCNIVC | | | TIVC | | | EAVC | | | FastVC | | |
|--------------------------|-----------------|------------------|----------------|----------------|-----------------|----------------|----------------|-----------------|----------------|----------------|----------------|----------------|
| | Min. | Avg. | T_Avg. | Min. | Avg. | T_Avg. | Min. | Avg. | T_Avg. | Min. | Avg. | T_Avg. |
| 144 | 117820 | 117844.5 | - | 117805 | 117836.9 | - | 117754 | 117836.9 | 780.352 | 117800 | 117810.6 | - |
| brock200-1 | 194 | 194 | 0.002 | 194 | 194 | < 0.001 | 194 | 194 | < 0.001 | 194 | 194 | < 0.001 |
| brock200-2 | 189 | 189 | 0.005 | 189 | 189 | 0.003 | 189 | 189 | 0.001 | 189 | 189 | < 0.001 |
| brock200-3 | 191 | 191 | 0.004 | 191 | 191 | < 0.001 | 191 | 191 | < 0.001 | 191 | 191 | 0.001 |
| brock200-4 | 192 | 192 | < 0.001 | 192 | 192 | < 0.001 | 192 | 192 | < 0.001 | 192 | 192 | < 0.001 |
| brock400-1 | 393 | 393 | 0.011 | 393 | 393 | 0.009 | 393 | 393 | 0.009 | 393 | 393 | 0.002 |
| brock400-2 | 392 | 392 | 0.15 | 392 | 392 | 0.105 | 392 | 392 | 0.051 | 392 | 392 | 0.024 |
| brock400-3 | 393 | 393 | 0.014 | 393 | 393 | 0.01 | 393 | 393 | 0.006 | 393 | 393 | < 0.001 |
| brock400-4 | 393 | 393 | 0.009 | 393 | 393 | 0.01 | 393 | 393 | 0.007 | 393 | 393 | 0.003 |
| brock800-1 | 790 | 790 | 3.18 | 790 | 790 | 1.028 | 790 | 790 | 0.373 | 790 | 790 | 0.071 |
| brock800-2 | 790 | 790 | 4.029 | 790 | 790 | 1.885 | 790 | 790 | 0.331 | 790 | 790 | 0.135 |
| brock800-3 | 789 | 789 | 70.521 | 789 | 789 | 50.873 | 789 | 789 | 3.472 | 789 | 789 | 789.4 |
| brock800-4 | 790 | 790 | 2.279 | 790 | 790 | 1.844 | 790 | 790 | 0.359 | 790 | 790 | 0.077 |
| 333SP | 2546845 | 2547438.9 | 999.825 | 2575912 | 2581720.3 | - | 2584618 | 2581720.3 | - | 2547802 | 2548294.8 | - |
| 598a | 89164 | 89179.9 | - | 89161 | 89177.9 | - | 89109 | 89177.9 | 711.32 | 89138 | 89147.3 | - |
| adaptive | 3407872 | 3407872 | 40.047 | 3407872 | 3407872 | 41.577 | 3407872 | 3407872 | 40.951 | 3407872 | 3407872 | 39.109 |
| al2010 | 138512 | 138520.6 | 532.095 | 138532 | 138547.4 | - | 138533 | 138547.4 | - | 138538 | 138551.1 | - |
| ar2010 | 102547 | 102551.8 | 460.306 | 102556 | 102566.4 | - | 102565 | 102566.4 | - | 102577 | 102586.1 | - |
| AS365 | 2629682 | 2630146.6 | 999.751 | 2631313 | 2632018.7 | - | 2631711 | 2632018.7 | - | 2631520 | 263172.1 | - |
| asia.osm | 5965052 | 5969310.3 | 999.998 | 6036476 | 6038513 | - | 6037354 | 6038513 | - | 5980801 | 5984162.5 | - |
| auto | 364594 | 364638.8 | - | 364493 | 364594.4 | 514.673 | 364647 | 364594.4 | - | 364808 | 364839.3 | - |
| az2010 | 132183 | 132195.7 | 308.63 | 1322215 | 132227.1 | - | 132215 | 132227.1 | - | 132237 | 132249.2 | - |
| belgium.osm | 716868 | 716875.1 | - | 716867 | 716881.5 | - | 716864 | 716881.5 | 883.474 | 716901 | 716922.2 | - |
| c-fat500-1 | 460 | 460 | < 0.001 | 460 | 460 | < 0.001 | 460 | 460 | 0.004 | 460 | 460 | < 0.001 |
| c-fat500-10 | 496 | 496 | 0.003 | 496 | 496 | 0.005 | 496 | 496 | 0.006 | 496 | 496 | 0.002 |
| c-fat500-2 | 480 | 480 | 0.002 | 480 | 480 | 0.002 | 480 | 480 | < 0.001 | 480 | 480 | 0.001 |
| c-fat500-5 | 492 | 492 | < 0.001 | 492 | 492 | < 0.001 | 492 | 492 | 0.001 | 492 | 492 | 0.001 |
| channel-500x100x100-b050 | 3601693 | 3604774.2 | - | 3601500 | 3601500 | 320.234 | 3601500 | 3601500 | 288.598 | 3601500 | 3601500 | 97.222 |
| citationCiteseer | 118133 | 118146.1 | 644.252 | 118134 | 118146.6 | - | 118135 | 118146.6 | - | 118177 | 118182.3 | - |
| co2010 | 110073 | 110083.5 | 744.358 | 110118 | 110134.2 | - | 110113 | 110134.2 | - | 110131 | 110149.1 | - |
| coAuthorsCiteseer | 129193 | 129193 | 1.959 | 129193 | 129193 | 1.376 | 129193 | 129193 | 1.12 | 129193 | 129193 | 3.825 |
| coAuthorsDBLP | 155618 | 155618 | 2.285 | 155618 | 155618 | 2.21 | 155618 | 155618 | 1.845 | 155618 | 155618 | 6.159 |
| com-Amzon | 160242 | 160246.2 | - | 160241 | 160246.1 | 192.983 | 160242 | 160246.1 | - | 160257 | 160258.6 | - |
| coPapersDBLP | 472179 | 472179 | 35.328 | 472179 | 472179 | 21.96 | 472179 | 472179 | 12.579 | 472179 | 472179 | 34.03 |
| cs4 | 13348 | 13348.4 | - | 13341 | 13346.1 | 843.164 | 13346 | 13346.1 | - | 13392 | 13398.8 | - |
| ct2010 | 37959.7 | 37959.7 | 474.844 | 37959 | 37960.6 | - | 37960 | 37960.6 | - | 37965 | 37966.9 | - |
| cti | 8779 | 8790.2 | - | 8752 | 8787.7 | 3.928 | 8769 | 8787.7 | - | 8769 | 8774.1 | - |
| data | 2163 | 2165.7 | 41.875 | 2163 | 2163 | 0.464 | 2163 | 2163 | 8.104 | 2163 | 2163 | 62.493 |
| de2010 | 13486 | 13487.5 | 512.72 | 13486 | 13486.9 | 475.093 | 13492 | 13486.9 | - | 13496 | 13498.5 | - |
| delaunay_n10 | 703 | 703 | 0.012 | 703 | 703 | 0.01 | 703 | 703 | 0.023 | 703 | 703 | 0.108 |
| delaunay_n11 | 1402 | 1402 | 0.114 | 1402 | 1402 | 0.041 | 1402 | 1402 | 0.235 | 1402 | 1402 | 8.948 |
| delaunay_n12 | 2807 | 2807.3 | 162.923 | 2807 | 2807.1 | 232.043 | 2807 | 2807.1 | 4.056 | 2807 | 2807 | 26.142 |
| delaunay_n13 | 5607 | 5607 | - | 5607 | 5607 | - | 5606 | 5607 | 358.952 | 5606 | 5606.6 | 281.008 |
| delaunay_n14 | 11228 | 11229.5 | - | 11229 | 11229.3 | - | 11227 | 11229.3 | 347.485 | 11227 | 11228.1 | 474.59 |
| delaunay_n15 | 22436 | 22437.2 | - | 22436 | 22436.8 | - | 22433 | 22436.8 | 538.58 | 22435 | 22438.5 | - |
| delaunay_n16 | 44847 | 44849.2 | - | 44846 | 44849.7 | - | 44841 | 44849.7 | 836.594 | 44848 | 44851.1 | - |
| delaunay_n18 | 179579 | 179587.1 | - | 179571 | 179580.5 | 654.066 | 179583 | 179580.5 | - | 179601 | 179610.1 | - |
| delaunay_n19 | 359123 | 359131.7 | - | 359109 | 359122.6 | 883.626 | 359116 | 359122.6 | - | 359149 | 359166.7 | - |
| delaunay_n20 | 718261 | 718289.1 | 992.751 | 718278 | 718305.3 | - | 718279 | 718305.3 | - | 718381 | 718397.5 | - |
| delaunay_n21 | 1436609 | 1436713.8 | 996.57 | 1436718 | 1436774.6 | - | 1436646 | 1436774.6 | - | 1437005 | 1437078.5 | - |
| delaunay_n22 | 2873905 | 2874225 | 999.491 | 2877230 | 2881724.6 | - | 2877438 | 2881724.6 | - | 2875899 | 2876043.8 | - |
| delaunay_n23 | 58331454 | 5833168.9 | 1000 | 5925261 | 592783.7 | - | 5919327 | 592783.7 | - | 5869161 | 5889915.5 | - |
| fe-4elt2 | 7572 | 7573.6 | - | 7571 | 7573.2 | 225.706 | 7571 | 7573.2 | 200.728 | 7572 | 7574.4 | - |
| fe-ocean | 72173 | 72235.1 | - | 72320 | 72985.2 | - | 72293 | 72985.2 | - | 72042 | 72580.2 | 792.088 |
| fe-rotor | 77615 | 77682.7 | - | 77613 | 77679.7 | - | 77598 | 77679.7 | 771.335 | 77609 | 77682.1 | - |
| fe-sphere | 10924 | 10924 | 1.617 | 10924 | 10924 | 0.178 | 10924 | 10924 | 0.146 | 10924 | 10924 | 0.128 |
| fe-tooth | 50344 | 50344 | - | 50344 | 50344 | - | 50343 | 50344 | 288.955 | 50344 | 50344.6 | - |
| fl2010 | 266945 | 266954.8 | 290.73 | 267014 | 267056.4 | - | 267020 | 267056.4 | - | 267069 | 267095.5 | - |
| ga2010 | 161677 | 161680.9 | 250.141 | 161699 | 161712 | - | 161706 | 161712 | - | 161715 | 161724.1 | - |
| germany.osm | 5707860 | 5713668.8 | 1000 | 5709765 | 5724860.9 | - | 5753918 | 5729861.6 | - | 5725595 | 5745895 | - |
| great-britain.osm | 3775495 | 3776049.4 | 999.622 | 3775634 | 3804688.1 | - | 3776498 | 3806603 | - | 3775969 | 3777278.8 | - |
| hi2010 | 13999 | 13999.1 | 395.53 | 14001 | 13999.5 | - | 14004 | 14006.3 | - | 13999 | 13999.5 | 379.535 |
| hugetrace-00000 | 2440871 | 2448230.7 | - | 2546693 | 2552111.8 | - | 2543741 | 2548412.1 | - | 2436844 | 2552111.8 | 1000 |
| hugetrace-00010 | 6907523 | 6912560.8 | - | 6932363 | 6934864.9 | - | 6935379 | 6937925.3 | - | 6862933 | 6934864.9 | 1000 |
| hugetrace-00020 | 9370177 | 9372996.8 | - | 9374264 | 9375672.3 | - | 9378885 | 9382696.8 | - | 9323551 | 9375672.3 | 1000 |
| hugetric-00000 | 3213841 | 3223599.8 | - | 3295606 | 3301469.9 | - | 3312151 | 3313985 | - | 3120767 | 3301469.9 | 1000 |
| hugetric-00010 | 3746758 | 3750856.7 | - | 3805083 | 3806746.9 | - | 3809329 | 3812190.9 | - | 3685757 | 3806746.9 | 1000 |
| hugetric-00020 | 4064777 | 4068062.5 | - | 4124266 | 4125926.6 | - | 4124033 | 4129304.8 | - | 3977727 | 4125926.6 | 1000 |
| ia-wiki-Talk | 17288 | 17288 | 0.214 | 17288 | < | | | | | | | |

Table 3: Experimental results on DAMACS10 continue.

| | luxembourg.osm | 56936 | 56937 | 288.412 | 56936 | 56937 | 504.936 | 56937 | 56938.1 | - | 56937 | 56937 | - |
|----------------------------|-----------------------|-------------------|----------------|----------------|----------------|----------------|---------------|-----------------|----------------|--------------|----------------|----------------|---|
| m14b | 175773 | 175792.8 | - | 175759 | 175791.2 | - | 175693 | 175713.9 | 884.959 | 175792 | 175791.2 | - | |
| M6 | 2423393 | 2423784.3 | 999.516 | 2424418 | 2426472.8 | - | 2424802 | 2425438.6 | - | 2424600 | 2426472.8 | - | |
| ma2010 | 87947 | 87955 | 482.958 | 87955 | 87961.2 | - | 87952 | 87963.9 | - | 87961 | 87961.2 | - | |
| md2010 | 77495 | 77498.7 | 538.144 | 77501 | 77507.3 | - | 77504 | 77510.5 | - | 77514 | 77507.3 | - | |
| me2010 | 37052 | 37053.4 | 545.704 | 37053 | 37055.7 | - | 37055 | 37059.7 | - | 37057 | 37055.7 | - | |
| mi2010 | 185819 | 185831.1 | 526.489 | 185880 | 185904 | - | 185899 | 185917.6 | - | 185906 | 185904 | - | |
| mm2010 | 144013 | 144029.8 | 363.04 | 144054 | 144080.4 | - | 144061 | 144093.5 | - | 144088 | 144080.4 | - | |
| mo2010 | 187679 | 187684.8 | 105.533 | 187710 | 187717.2 | - | 187695 | 187717 | - | 187741 | 187717.2 | - | |
| ms2010 | 94936 | 94940.1 | 550.15 | 94944 | 94955.8 | - | 94947 | 94956.8 | - | 94955 | 94955.8 | - | |
| mt2010 | 70631 | 70643.3 | 521.483 | 70641 | 70659.8 | - | 70652 | 70670.6 | - | 70652 | 70659.8 | - | |
| nc2010 | 159831 | 159836.8 | 68.561 | 159859 | 159870.4 | - | 159860 | 159872.3 | - | 159867 | 159870.4 | - | |
| nd2010 | 73681 | 73689.9 | 681.222 | 73711 | 73719.3 | - | 73720 | 73724.4 | - | 73716 | 73719.3 | - | |
| ne2010 | 108184 | 108194.7 | 641.721 | 108232 | 108246 | - | 108237 | 108254.1 | - | 108277 | 108246 | - | |
| netherlands.osm | 1100047 | 1100056.7 | 961.626 | 1100083 | 1100095.7 | - | 1100084 | 1100093.6 | - | 1100136 | 1100095.7 | - | |
| nh2010 | 25956 | 25956.4 | 532.643 | 25956 | 25956.6 | 595.811 | 25957 | 25961.3 | - | 25957 | 25956 | - | |
| nj2010 | 96795 | 96800.1 | 626.151 | 96828 | 96839.9 | - | 96830 | 96842.1 | - | 96838 | 96839.9 | - | |
| NLR | 2881932 | 2882387.4 | 999.65 | 2895352 | 2906568.7 | - | 2888773 | 2894395.6 | - | 2883577 | 2906568.7 | - | |
| nm2010 | 91765 | 91772.8 | 456.312 | 91784 | 91792.7 | - | 91781 | 91795.6 | - | 91797 | 91792.7 | - | |
| nv2010 | 46157 | 46163.4 | 736.28 | 46161 | 46166.7 | - | 46166 | 46174.1 | - | 46184 | 46166.7 | - | |
| oh2010 | 205441 | 205452.2 | 632.067 | 205492 | 205518.9 | - | 205500 | 205515.2 | - | 205530 | 205518.9 | - | |
| ok2010 | 147566 | 147582.6 | 600.037 | 147631 | 147662.5 | - | 147635 | 147662.3 | - | 147682 | 147662.5 | - | |
| or2010 | 107622 | 107629.5 | 420.516 | 107637 | 107656.7 | - | 107648 | 107656.9 | - | 107675 | 107656.7 | - | |
| p-hat700-3 | 690 | 690 | 1.167 | 690 | 690 | 0.578 | 690 | 690 | 0.13 | 690 | 690 | 0.029 | |
| preferentialAttachment | 57899 | 57901.4 | - | 57895 | 57899.3 | 564.193 | 57895 | 57898.6 | 572.747 | 57895 | 57899.3 | 560.209 | |
| ri2010 | 14377 | 14377.5 | 475.117 | 14377 | 14378 | 677.768 | 14381 | 14383.8 | - | 14384 | 14378 | - | |
| road_central | 6885046 | 6862104.2 | 1000 | 705150 | 7055778.8 | - | 7049103 | 7051093.7 | - | 7050693 | 7055778.8 | - | |
| road_usa | 11772344 | 11773699.8 | 1000 | 12077392 | 12079749.5 | - | 12074967 | 12077887.9 | - | 12122686 | 12079749.5 | - | |
| sc2010 | 100844 | 100850.9 | 475.374 | 100855 | 100862.6 | - | 100859 | 100866.8 | - | 100870 | 100862.6 | - | |
| sd2010 | 49302 | 49316.9 | 852.058 | 49326 | 49334.7 | - | 49348 | 49359.2 | - | 49352 | 49334.7 | - | |
| smallworld | 75541 | 75553.4 | - | 75532 | 75538.3 | 982.666 | 75609 | 75624.2 | - | 75665 | 75538.3 | - | |
| t60k | 30324 | 30332 | 50.33 | 30332 | 30332 | - | 30332 | 30332 | - | 30332 | 30332 | - | |
| tn2010 | 134349 | 134355.4 | 275.611 | 134358 | 134364.8 | - | 134356 | 134367.2 | - | 134377 | 134364.8 | - | |
| tx2010 | 512894 | 512922.4 | 593.468 | 513117 | 513168.1 | - | 513114 | 513154.1 | - | 513222 | 513168.1 | - | |
| uk | 2626 | 2626 | 115.868 | 2626 | 2626 | 52.965 | 2626 | 2626.6 | 438.331 | 2626 | 2626 | - | |
| ut2010 | 62142 | 62147.6 | 708.633 | 62155 | 62159.9 | - | 62158 | 62164.7 | - | 62164 | 62159.9 | - | |
| va2010 | 154257 | 154263.4 | 336.302 | 154270 | 154277.3 | - | 154272 | 154281.7 | - | 154291 | 154277.3 | - | |
| venturiLevel3 | 2026295 | 2026301.9 | 877.714 | 2026353 | 2026363.9 | - | 2026354 | 2026359.4 | - | 2026352 | 2026363.9 | - | |
| vsp_scatp1-2b_and_seymourl | 17784 | 17785.1 | 573.491 | 17785 | 17785.2 | - | 17787 | 17787.3 | - | 17787 | 17785.2 | - | |
| vt2010 | 17461 | 17461.1 | 516.454 | 17461 | 17461.5 | 566.526 | 17462 | 17464.1 | - | 17465 | 17461.5 | - | |
| wa2010 | 108793 | 108799.2 | 616.691 | 108832 | 108841.1 | - | 108830 | 108847.1 | - | 108861 | 108841.1 | - | |
| wi2010 | 141664 | 141679.1 | 382.336 | 141704 | 141726.5 | - | 141707 | 141725.2 | - | 141729 | 141726.5 | - | |
| wing | 36879 | 36897.7 | - | 36867 | 36886.8 | 981.95 | 36975 | 36990.2 | - | 37010 | 36886.8 | - | |
| wing_nodal | 8807 | 8808.5 | - | 8806 | 8808.1 | - | 8801 | 8802.6 | - | 8800 | 8808.1 | 482.861 | |
| wv2010 | 71166 | 71170 | 436.763 | 71170 | 71179 | - | 71167 | 71181.6 | - | 71178 | 71179 | - | |
| wy2010 | 46748 | 46752.1 | 678.237 | 46748 | 46754.7 | 847.438 | 46756 | 46762.9 | - | 46775 | 46754.7 | - | |

Table 4: Experimental results on SNAP

| Instance | GCNIVC | | | TIVC | | | EAVC | | | FastVC | | | |
|--------------------|---------------|-----------------|----------------|---------------|----------------|----------------|---------------|---------------|---------------|---------------|----------------|--------------|--------|
| | Min. | Avg. | T.Avg. | Min. | Avg. | T.Avg. | Min. | Avg. | T.Avg. | Min. | Avg. | T.Avg. | |
| ca-MathSciNet | 139951 | 139951 | 4.97 | 139951 | 139951 | 4.992 | 139951 | 139951 | 3.288 | 139951 | 139951 | 11.567 | |
| c-fat200-1 | 182 | 182 | <0.001 | 182 | 182 | <0.001 | 182 | 182 | <0.001 | 182 | 182 | <0.001 | |
| c-fat200-2 | 191 | 191 | <0.001 | 191 | 191 | <0.001 | 191 | 191 | <0.001 | 191 | 191 | <0.001 | |
| c-fat200-5 | 197 | 197 | <0.001 | 197 | 197 | 0.003 | 197 | 197 | 0.002 | 197 | 197 | <0.001 | |
| com-DBLP | 164949 | 164949 | 3.177 | 164949 | 164949 | 2.463 | 164949 | 164949 | 3.035 | 164949 | 164949 | 13.43 | |
| co-papers-citeseer | 386106 | 386106 | 21.105 | 386106 | 386106 | 12.645 | 386106 | 386106 | 10.851 | 386106 | 386106 | 38.388 | |
| ia2010 | 123075 | 123087.7 | 670.688 | 123198 | 123206.9 | - | 123126 | 123144.6 | - | 123152 | 123163.3 | - | |
| ia-reality | 81 | 81 | 0.002 | 81 | 81 | 0.002 | 81 | 81 | 0.003 | 81 | 81 | <0.001 | |
| loc-Brightkite | 21867 | 21867.1 | 116.11 | 21867 | 21867 | 102.738 | 21867 | 21867.2 | 58.983 | 21867 | 21867 | 0.427 | |
| loc-Gowalla | 84222 | 84222.7 | 111.621 | 84222 | 84222 | 84222.6 | 64.972 | 84222 | 84222.5 | 25.892 | 84222 | 84222.6 | 85.634 |
| ca-netscience | 214 | 214 | <0.001 | 214 | 214 | <0.001 | 214 | 214 | <0.001 | 214 | 214 | <0.001 | |
| ca-HepPh | 6555 | 6555 | 0.041 | 6555 | 6555 | 0.03 | 6555 | 6555 | 0.034 | 6555 | 6555 | 0.025 | |
| caidaRouterLevel | 75193 | 75209.6 | - | 75189 | 75204.6 | 887.406 | 75194 | 75214.2 | - | 75432 | 75204.6 | - | |

highlights each algorithm's performance within an acceptable solution space, facilitating a more nuanced comparison of their convergence speeds and the quality of their final solutions.

Given the outstanding performance of our GCNIVC on the DIMACS10 benchmark regarding solution quality, we evaluated the convergence speed of solutions on instances from this benchmark. We compared four algorithms across four instances for our testing, where graphs were selected based on varying sizes, specifically two large graphs with a size of 10^6 (Figures 2 (a)

and (b)) and two smaller graphs with a size of 10^5 (Figures 2 (c) and (d)). Figure 2 presents the convergence curves of these algorithms across the four graphs, with the x-axis representing time and the y-axis indicating the size of a VC. Due to the large number of vertices in the graphs shown in Figures 2 (a) and (b), the convergence curves provide clear differentiation for analyzing the algorithms' performance. By establishing a higher upper bound threshold (denoted as 5,892,463 for Figure 2 (a) and 3,853,211 for Figure 2 (b)), we can observe the rapid convergence process of these algorithms in the

Table 5: Experimental results on Gset

| Instance | GCNIVC | | | TIVC | | | EAVC | | | FastVC | | |
|----------|-------------|-------------|---------|-------------|-------------|---------------|-------------|--------------|--------------|-------------|-------------|---------|
| | Min. | Avg. | T_Avg. | Min. | Avg. | T_Avg. | Min. | Avg. | T_Avg. | Min. | Avg. | T_Avg. |
| G1 | 705 | 705 | 0.553 | 705 | 705 | 0.172 | 705 | 0.093 | | 705 | 705 | 1.1 |
| G14 | 521 | 521 | 0.006 | 521 | 521 | 0.002 | 521 | 521 | 0.005 | 521 | 521 | 0.105 |
| G15 | 517 | 517 | 0.006 | 517 | 517 | 0.002 | 517 | 517 | <0.001 | 517 | 517 | 0.002 |
| G16 | 515 | 515 | <0.001 | 515 | 515 | <0.001 | 515 | 515 | <0.001 | 515 | 515 | <0.001 |
| G17 | 514 | 514 | 0.012 | 514 | 514 | 0.007 | 514 | 514 | 0.009 | 514 | 514 | 0.017 |
| G2 | 706 | 706 | 0.51 | 706 | 706 | 0.484 | 706 | 706 | 0.06 | 706 | 706 | 0.139 |
| G22 | 1567 | 1567 | 5.965 | 1567 | 1567 | 2.743 | 1567 | 1567 | 80.451 | 1567 | 1567 | 470.18 |
| G23 | 1573 | 1573 | 125.242 | 1573 | 1573 | 97.096 | 1573 | 1573 | 1573.5 | 1573 | 1573 | 336.577 |
| G24 | 1569 | 1569 | 55.064 | 1569 | 1569 | 18.007 | 1569 | 1569 | 140.438 | 1569 | 1569 | 207.84 |
| G25 | 1570 | 1570 | 3.114 | 1570 | 1570 | 1.156 | 1570 | 1570 | 9.608 | 1570 | 1570 | 26.736 |
| G26 | 1573 | 1573 | 4.698 | 1573 | 1573 | 1.563 | 1573 | 1573 | 1573.1 | 1573 | 1573 | 98.189 |
| G3 | 706 | 706 | 0.787 | 706 | 706 | 0.182 | 706 | 706 | 0.114 | 706 | 706 | 0.677 |
| G35 | 1282 | 1282 | 0.009 | 1282 | 1282 | 0.003 | 1282 | 1282 | 0.005 | 1282 | 1282 | 0.018 |
| G36 | 1304 | 1304 | 0.016 | 1304 | 1304 | 0.011 | 1304 | 1304 | 0.011 | 1304 | 1304 | 0.017 |
| G37 | 1292 | 1292 | 0.016 | 1292 | 1292 | 0.014 | 1292 | 1292 | 0.005 | 1292 | 1292 | 0.036 |
| G38 | 1284 | 1284 | 0.002 | 1284 | 1284 | <0.001 | 1284 | 1284 | 0.001 | 1284 | 1284 | 0.01 |
| G4 | 705 | 705 | 3.448 | 705 | 705 | 3.317 | 705 | 705 | 0.182 | 705 | 705 | 0.503 |
| G43 | 787 | 787 | 1.165 | 787 | 787 | 0.705 | 787 | 787 | 0.858 | 787 | 787 | 53.642 |
| G44 | 786 | 786 | 0.156 | 786 | 786 | 0.146 | 786 | 786 | 0.137 | 786 | 786 | 2.54 |
| G45 | 789 | 789 | 0.327 | 789 | 789 | 0.159 | 789 | 789 | 0.476 | 789 | 789 | 6.955 |
| G46 | 789 | 789 | 2.632 | 789 | 789 | 1.041 | 789 | 789 | 3.343 | 789 | 789 | 43.772 |
| G47 | 785 | 785 | 1.144 | 785 | 785 | 0.559 | 785 | 785 | 16.804 | 785 | 785 | 187.001 |
| G48 | 1500 | 1500 | <0.001 | 1500 | 1500 | 0.001 | 1500 | 1500 | 0.005 | 1500 | 1500 | <0.001 |
| G49 | 1500 | 1500 | 0.003 | 1500 | 1500 | 0.003 | 1500 | 1500 | 0.004 | 1500 | 1500 | <0.001 |
| G5 | 706 | 706 | 2.638 | 706 | 706 | 0.962 | 706 | 706 | 0.179 | 706 | 706 | 0.722 |
| G50 | 1560 | 1560 | 0.004 | 1560 | 1560 | 0.003 | 1560 | 1560 | 0.001 | 1560 | 1560 | <0.001 |
| G51 | 651 | 651 | 0.003 | 651 | 651 | 0.002 | 651 | 651 | 0.005 | 651 | 651 | <0.001 |
| G52 | 652 | 652 | 0.007 | 652 | 652 | 0.002 | 652 | 652 | 0.003 | 652 | 652 | <0.001 |
| G53 | 653 | 653 | 0.082 | 653 | 653 | 0.099 | 653 | 653 | 0.059 | 653 | 653 | 0.184 |
| G54 | 659 | 659 | 0.009 | 659 | 659 | 0.004 | 659 | 659 | 0.006 | 659 | 659 | 0.006 |
| G58 | 3218 | 3218 | 2.225 | 3218 | 3218 | 1.236 | 3218 | 3218 | 0.25 | 3218 | 3218 | 1.935 |
| G63 | 4507 | 4507 | 0.22 | 4507 | 4507 | 0.216 | 4507 | 4507 | 0.1 | 4507 | 4507 | 0.519 |

early stages. In contrast, the graphs in Figures 2 (c) and (d) have a smaller scale. Therefore, the convergence curves exhibit a steep decline in the initial stages, followed by a less pronounced stabilization phase. To better illuminate this behavior, we apply an upper bound threshold (designated as 261,250 for Figure 2 (c) and 123,300 for Figure 2 (d)).

The findings presented in Figure 2 (a) and Figure 2 (b) illustrate that the GCNIVC algorithm effectively employs the GCN-based initialization method to attain an optimal initial solution. This solution surpasses those obtained by the FastVC, EAVC, and TIVC algorithms, which require additional processing times to refine their results through heuristic search procedures. As a result, the GCNIVC algorithm saves more time for subsequent heuristic searches. For instance, in Figure 2 (a), the GCNIVC algorithm successfully reduces the solution size from 5,830,163 vertices to 5,735,000 vertices in just 91 seconds. In comparison, the TIVC algorithm necessitates 1,000 seconds to achieve the same reduction, while the EAVC algorithm takes approximately 684 seconds, and FastVC requires around 230 seconds. Similarly, in Figure 2 (b), the GCNIVC algorithm decreases the solution size from 3,853,211 vertices to 3,780,000 in about 65 seconds. In contrast, the TIVC algorithm takes

roughly 414 seconds, the EAVC algorithm takes around 374 seconds, and FastVC takes approximately 143 seconds to reach the same result.

When working with relatively smaller graphs, all algorithms quickly converge at the beginning. In Figure 2 (c), they enter a slow improvement phase after about 200 seconds. GCNIVC gets a solution size of 261,008 during this phase, while FastVC, TIVC, and EAVC reach 261,223, 261,177, and 261,184, respectively. GCNIVC provides the best quality solution at the start of this slow phase. Then, GCNIVC reduces its solution size to 261,001, while FastVC, TIVC, and EAVC reduce their solution sizes to 261,217, 261,167, and 261,183, respectively. Thus, the reductions in solution sizes during this slow improvement phase are seven for GCNIVC, six for FastVC, ten for TIVC, and one for EAVC. Similarly, Figure 2 (d) shows that the algorithms enter the slow improvement phase in just 5 seconds. Currently, GCNIVC has a solution size of 123,089, while FastVC, TIVC, and EAVC produce sizes of 123,199, 123,150, and 123,152, respectively. Again, GCNIVC offers the best solution at the start of the slow phase. After this phase, GCNIVC reduces its size to 123,075, while FastVC, TIVC, and EAVC achieve sizes of 123,198, 123,126, and 123,152, respectively. There-

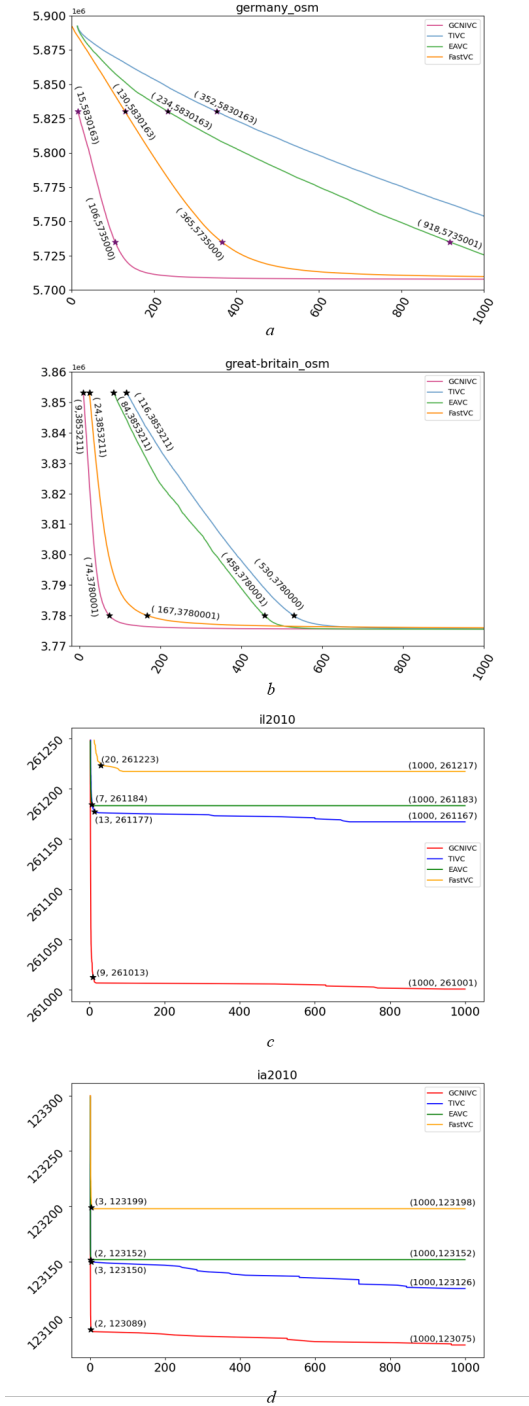


Figure 2: The decreasing trend of using different heuristic search algorithms over 1000 seconds on benchmark tests.

fore, the reductions in solution size during this phase are 14 for GCNIVC, 0 for FastVC, 24 for TIVC, and 0

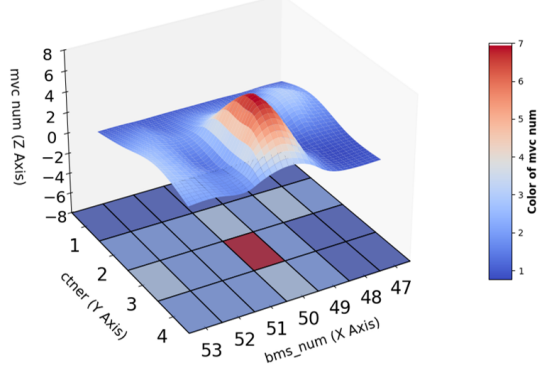


Figure 3: Results of parameter tuning.

for EAVC. This indicates that although TIVC performs slightly better during the slow improvement period, GCNIVC shows the best convergence speed in the whole period.

5.3.3. Parameter tuning

We experimented to optimize the parameters $ctner$ and bms_num in GCNIVC (Algorithm 3). For this, we selected 19 instances from various benchmarks, with the number of vertices ranging from 10^5 to 10^7 . We assessed the performance of GCNIVC across 28 different combinations associated with these two parameters, where $ctner$ took values from {1, 2, 3, 4} and bms_num varied within the range {47, 48, 49, 50, 51, 52, 53}, following the experimental setup detailed in Section 5.2. For each configuration, we executed GCNIVC with fixed values of $ctner$ and bms_num , utilizing ten different random seeds, and reported the best results.

Figure 3 showcases the experimental results, with the x-axis denoting bms_num , the y-axis representing $ctner$, and the z-axis indicating the number of instances in which an optimal solution (i.e., an MVC) is achieved. The 3D surface plot above the $z = 0$ plane clearly visualizes how various combinations influence the number of optimal solutions obtained. In this plot, higher z -values signify a greater number of optimal solutions, with the peak of the surface representing the optimal combination, where the planar plot at $z = -8$ illustrates the color distribution for each combination of $ctner$ and bms_num . A deeper red hue reflects a higher count of optimal solutions that combination attained. As depicted in Figure 3, GCNIVC achieved optimal solutions for seven instances with $ctner = 3$ and $bms_num = 50$. This combination represents the highest number of in-

stances effectively resolved by GCNIVC in this experiment. Consequently, we selected $ctner = 3$ and $bms_num = 50$ as the optimal parameters for GCNIVC.

5.3.4. Initial solutions

Table 8-9 (see Appendix) presents the sizes of initial solutions generated by GreedyConstructVC and GCNConstructVC across 302 benchmark instances. The data demonstrates that GCNConstructVC outperforms GreedyConstructVC. Specifically, GCNConstructVC yielded superior initial solutions in 178 instances, while GreedyConstructVC excelled in 68 instances. These findings highlight the considerable advantage of GCNConstructVC in generating high-quality initial solutions.

5.3.5. Ablation experiments

We conducted an ablation study to assess the impact of various components on the overall performance of the GCNIVC algorithm. In this study, we removed the CRV strategy (Algorithm 2) from GCNIVC (line 7 in Algorithm 3) and the double-covered number technique (Definition 1) from GCNIVC (lines 9 and 18 in Algorithm 3), resulting in two new algorithms designated as No_CRV and No_Dcnumber, respectively. We used ten random seeds to compare GCNIVC with No_CRV and No_Dcnumber across the 302 graphs from the four testing benchmarks. It is important to emphasize that since small graphs can frequently yield optimal solutions, we focused exclusively on larger graphs and reported results only for instances where the two compared algorithms generated different solutions. Table 10 (see Appendix) summarizes the experimental results for No_CRV versus GCNIVC. The findings reveal that GCNIVC outperformed No_CRV in 77 instances, while No_CRV produced better solutions in 8 cases. Likewise, Table 11 (see Appendix) presents the results of the comparison between No_Dcnumber and GCNIVC, showing that GCNIVC outperformed No_Dcnumber in 81 instances, while No_Dcnumber achieved superior solutions in 5 cases. This comparative analysis concludes that both components significantly enhance the algorithm's performance, particularly when combined. Nonetheless, each component positively contributes to the overall results.

5.3.6. Discussion

The exceptional performance of GCNIVC can be attributed to several key factors. Firstly, the impressive enhancement in heuristic search algorithms is mainly due to the rapid convergence speed of GCNConstruct. This quick convergence facilitates the generation of

high-quality initial solutions faster, allowing more time for subsequent searches to refine the ultimate solution's quality. Moreover, by incorporating the CRV heuristic, which is based on three containers and the concept of double-covered edges, GCNIVC can dynamically adjust removal operations throughout the solution search phase. This adaptability greatly enhances GCNIVC's ability to improve the quality of the final solution. These insights thoroughly explain why GCNIVC consistently achieves outstanding performance across benchmark instances.

6. Conclusion and Future Work

We have developed an efficient heuristic search algorithm, GCNIVC, designed to address the MVC problem. This algorithm employs the GCN framework during its initialization phase, allowing for effective analysis of graph structures and generating a high-quality initial solution. Additionally, GCNIVC introduces a novel concept known as double-covered edges, which aids in vertex selection. This enhancement boosts search efficiency by offering increased flexibility in adding and removing operations based on the attributes of edges. Our extensive experimental results demonstrate that GCNIVC outperforms other state-of-the-art MVC algorithms across four benchmark datasets, encompassing 302 instances. This performance improvement underscores the algorithm's effectiveness in handling the MVC problem on large-scale graphs.

In our future work, we aspire to expand the application of these techniques to solve other intractable graph problems involving large-scale graphs, such as the minimum dominating set problem. In addition, we plan to explore more methodologies for incorporating advanced machine-learning techniques into the heuristic search framework. Our goals include enhancing the quality of initial solutions even further and optimizing the convergence speed of the algorithm to make it more efficient in practical applications.

References

- [1] D. Coppersmith, U. Vishkin, Solving np-hard problems in 'almost trees': Vertex cover, *Discret. Appl. Math.* 10 (1) (1985) 27–45.
- [2] I. Dinur, S. Safra, On the hardness of approximating minimum vertex cover, *Annals of mathematics* (2005) 439–485.
- [3] C. Liu, S. Ge, Y. Zhang, Identifying the cardinality-constrained critical nodes with a hybrid evolutionary algorithm, *Inf. Sci.* 642 (2023) 119140.
- [4] T. Akiba, Y. Iwata, Branch-and-reduce exponential/fpt algorithms in practice: A case study of vertex cover, *Theoretical Computer Science* 609 (2016) 211–225.

- [5] J. Chen, I. A. Kanj, G. Xia, Improved upper bounds for vertex cover, *Theoretical Computer Science* 411 (40-42) (2010) 3736–3756.
- [6] Y. Li, M. T. Thai, F. Wang, C.-W. Yi, P.-J. Wan, D.-Z. Du, On greedy construction of connected dominating sets in wireless networks, *Wireless Communications and Mobile Computing* 5 (8) (2005) 927–932.
- [7] S. Bouamama, C. Blum, A. Boukerram, A population-based iterated greedy algorithm for the minimum weight vertex cover problem, *Applied Soft Computing* 12 (6) (2012) 1632–1639.
- [8] T. A. Feo, M. G. Resende, S. H. Smith, A greedy randomized adaptive search procedure for maximum independent set, *Operations Research* 42 (5) (1994) 860–878.
- [9] Q. Han, H. Sang, Q. Pan, B. Zhang, H. Guo, An efficient collaborative multi-swap iterated greedy algorithm for the distributed permutation flowshop scheduling problem with preventive maintenance, *Swarm Evol. Comput.* 86 (2024) 101537. doi:10.1016/J.SWEVO.2024.101537. URL <https://doi.org/10.1016/j.swevo.2024.101537>
- [10] M. S. Viana, O. M. Junior, R. C. Contreras, A modified genetic algorithm with local search strategies and multi-crossover operator for job shop scheduling problem, *Sensors* 20 (18) (2020) 5440.
- [11] E. Zhu, F. Jiang, C. Liu, J. Xu, Partition independent set and reduction-based approach for partition coloring problem, *IEEE Trans. Cybern.* 52 (6) (2022) 4960–4969.
- [12] B. Zhao, H. Lu, S. Chen, J. Liu, D. Wu, Convolutional neural networks for time series classification, *Journal of systems engineering and electronics* 28 (1) (2017) 162–169.
- [13] J. Xie, L. Gao, X. Li, L. Gui, A hybrid genetic tabu search algorithm for distributed job-shop scheduling problems, *Swarm Evol. Comput.* 90 (2024) 101670. doi:10.1016/J.SWEVO.2024.101670. URL <https://doi.org/10.1016/j.swevo.2024.101670>
- [14] S. Tian, C. Zhang, J. Fan, X. Li, L. Gao, A genetic algorithm with critical path-based variable neighborhood search for distributed assembly job shop scheduling problem, *Swarm Evol. Comput.* 85 (2024) 101485. doi:10.1016/J.SWEVO.2024.101485. URL <https://doi.org/10.1016/j.swevo.2024.101485>
- [15] C. Liu, G. Liu, C. Luo, S. Cai, Z. Lei, W. Zhang, Y. Chu, G. Zhang, Optimizing local search-based partial maxsat solving via initial assignment prediction, *Science China Information Sciences* 68 (2025).
- [16] S. Cai, Balance between complexity and quality: Local search for minimum vertex cover in massive graphs, in: *Twenty-Fourth International Joint Conference on Artificial Intelligence*, 2015.
- [17] S. Cai, K. Su, C. Luo, A. Sattar, Numvc: An efficient local search algorithm for minimum vertex cover, *Journal of Artificial Intelligence Research* 46 (2013) 687–716.
- [18] S. Richter, M. Helmert, C. Gretton, A stochastic local search approach to vertex cover, in: J. Hertzberg, M. Beetz, R. Englert (Eds.), *KI 2007: Advances in Artificial Intelligence*, 30th Annual German Conference on AI, KI 2007, Osnabrück, Germany, September 10-13, 2007, Proceedings, Vol. 4667 of Lecture Notes in Computer Science, Springer, 2007, pp. 412–426.
- [19] S. Cai, K. Su, A. Sattar, Local search with edge weighting and configuration checking heuristics for minimum vertex cover, *Artif. Intell.* 175 (9-10) (2011) 1672–1696.
- [20] Z. Ma, Y. Fan, K. Su, C. Li, A. Sattar, Local search with noisy strategy for minimum vertex cover in massive graphs, in: R. Booth, M. Zhang (Eds.), *PRICAI 2016: Trends in Artificial Intelligence - 14th Pacific Rim International Conference on Artificial Intelligence*, Phuket, Thailand, August 22–26, 2016, Proceedings, Vol. 9810 of Lecture Notes in Computer Science, Springer, 2016, pp. 283–294.
- [21] S. Cai, J. Lin, C. Luo, Finding A small vertex cover in massive sparse graphs: Construct, local search, and preprocess, *J. Artif. Intell. Res.* 59 (2017) 463–494.
- [22] C. Luo, H. H. Hoos, S. Cai, Q. Lin, H. Zhang, D. Zhang, Local search with efficient automatic configuration for minimum vertex cover., in: *IJCAI*, 2019, pp. 1297–1304.
- [23] C. Quan, P. Guo, A local search method based on edge age strategy for minimum vertex cover problem in massive graphs, *Expert Systems with Applications* 182 (2021) 115185.
- [24] Y. Zhang, S. Wang, C. Liu, E. Zhu, Tive: An efficient local search algorithm for minimum vertex cover in large graphs, *Sensors* 23 (18) (2023) 7831.
- [25] Y. Rong, W. Huang, T. Xu, J. Huang, Dropedge: Towards deep graph convolutional networks on node classification, in: *8th International Conference on Learning Representations*, ICLR 2020, Addis Ababa, Ethiopia, April 26-30, 2020, OpenReview.net, 2020.
- [26] A. Tsitsulin, J. Palowitch, B. Perozzi, E. Müller, Graph clustering with graph neural networks, *J. Mach. Learn. Res.* 24 (2023) 127:1–127:21.
- [27] L. Wang, S. Hu, M. Li, J. Zhou, An exact algorithm for minimum vertex cover problem, *Mathematics* 7 (7) (2019).
- [28] D. A. Bader, H. Meyerhenke, P. Sanders, D. Wagner, *Graph partitioning and graph clustering*, Vol. 588, American Mathematical Society Providence, RI, 2013.
- [29] S. J. Benson, Y. Ye, X. Zhang, Mixed linear and semidefinite programming for combinatorial and quadratic optimization, *Optimization Methods and Software* 11 (1-4) (1999) 515–544.

Appendix

See Tables 6 and 11.

Table 6: Experimental results on Network Repository

| Instance | GCNIVC | | | TIVC | | | EAVC | | | FastVC | | |
|---------------------|---------------|---------------|----------------|---------------|-----------------|----------------|------------------|---------------|---------------|---------------|-----------------|--------------|
| | Min. | Avg. | T_Avg. | Min. | Avg. | T_Avg. | Min. | Avg. | T_Avg. | Min. | Avg. | T_Avg. |
| p-hat1000-1 | 925 | 925 | 6.672 | 925 | 925 | 2.984 | 925 | 925 | 0.073 | 925 | 925 | 0.031 |
| p-hat1000-2 | 946 | 946 | 1.087 | 946 | 946 | 0.339 | 946 | 946 | 0.047 | 946 | 946 | 0.009 |
| p-hat1500-1 | 1413 | 1413 | 6.725 | 1413 | 1413 | 3.272 | 1413 | 1413 | 0.117 | 1413 | 1413 | 0.042 |
| p-hat1500-2 | 1438 | 1438 | 1.12 | 1438 | 1438 | 0.342 | 1438 | 1438 | 0.081 | 1438 | 1438 | 0.019 |
| p-hat1500-3 | 1488 | 1488.2 | 249.719 | 1488 | 1488.1 | 303.954 | 1488 | 1488.3 | 24.333 | 1488 | 1488.1 | 4.391 |
| p-hat300-3 | 291 | 291 | 0.013 | 291 | 291 | 0.008 | 291 | 291 | 0.006 | 291 | 291 | 0.001 |
| p-hat500-2 | 464 | 464 | 0.017 | 464 | 464 | 0.012 | 464 | 464 | 0.009 | 464 | 464 | 0.001 |
| p-hat500-3 | 490 | 490 | 0.154 | 490 | 490 | 0.037 | 490 | 490 | 0.023 | 490 | 490 | 0.015 |
| p-hat700-1 | 635 | 635 | 0.027 | 635 | 635 | 0.013 | 635 | 635 | 0.01 | 635 | 635 | 0.001 |
| p-hat700-2 | 651 | 651 | 0.03 | 651 | 651 | 0.022 | 651 | 651 | 0.017 | 651 | 651 | 0.001 |
| san1000 | 933 | 933 | 0.039 | 933 | 933 | 0.035 | 933 | 933 | 0.039 | 933 | 933 | 0.004 |
| san200-0-7-1 | 191 | 191 | 0.02 | 191 | 191 | 0.01 | 191 | 191 | 0.006 | 191 | 191 | 0.027 |
| san200-0-7-2 | 188 | 188 | <0.001 | 188 | 188 | <0.001 | 188 | 188 | <0.001 | 188 | 188 | <0.001 |
| san200-0-9-1 | 196 | 196 | 0.004 | 196 | 196 | 0.005 | 196 | 196 | 0.002 | 196 | 196 | 0.001 |
| san200-0-9-2 | 196 | 196 | 0.004 | 196 | 196 | 0.003 | 196 | 196 | 0.001 | 196 | 196 | <0.001 |
| san200-0-9-3 | 195 | 195 | 0.004 | 195 | 195 | 0.005 | 195 | 195 | 0.002 | 195 | 195 | <0.001 |
| san400-0-5-1 | 368 | 368 | <0.001 | 368 | 368 | 0.001 | 368 | 368 | 0.002 | 368 | 368 | 0.001 |
| san400-0-7-1 | 389 | 389 | 0.013 | 389 | 389 | 0.007 | 389 | 389 | 0.002 | 389 | 389 | <0.001 |
| san400-0-7-2 | 385 | 385 | 1.061 | 385 | 385 | 0.634 | 385 | 385.3 | 0.059 | 385 | 385 | 0.487 |
| san400-0-7-3 | 381 | 381 | 0.01 | 381 | 381.6 | 19.33 | 382 | 382 | - | 381 | 381.6 | <0.001 |
| san400-0-9-1 | 395 | 395 | 0.013 | 395 | 395 | 0.01 | 395 | 395 | 0.01 | 395 | 395 | 0.002 |
| sanr200-0-7 | 193 | 193 | 0.001 | 193 | 193 | <0.001 | 193 | 193 | <0.001 | 193 | 193 | <0.001 |
| sanr200-0-9 | 196 | 196 | 0.003 | 196 | 196 | 0.003 | 196 | 196 | 0.003 | 196 | 196 | <0.001 |
| sanr400-0-5 | 387 | 387 | 0.465 | 387 | 387 | 0.154 | 387 | 387 | 0.061 | 387 | 387 | 0.055 |
| sanr400-0-7 | 392 | 392 | 0.038 | 392 | 392 | 0.024 | 392 | 392 | 0.007 | 392 | 392 | 0.001 |
| scc_infect-dublin | 9103 | 9103 | 0.082 | 9103 | 9103 | 2.795 | 9103 | 9103 | 67.958 | 9104 | 9103 | - |
| scc_infect-hyper | 110 | 110 | 0.001 | 110 | 110 | <0.001 | 110 | 110 | <0.001 | 110 | 110 | <0.001 |
| scc_reality | 2486 | 2486 | 0.649 | 2486 | 2486 | 0.622 | 2486 | 2486 | 0.627 | 2486 | 2486 | 0.119 |
| soc-BlogCatalog | 20752 | 20752 | 1.128 | 20752 | 20752 | 0.812 | 20752 | 20752 | 0.583 | 20752 | 20752 | 0.469 |
| soc-brightkite | 21190 | 21190 | 54.289 | 21190 | 21190 | 58.291 | 21190 | 21190.3 | 82.545 | 21190 | 21190 | 0.457 |
| soc-buzznet | 30618 | 30621.5 | - | 30615 | 30620.1 | 321.467 | 30624 | 30624 | - | 30625 | 30620.1 | - |
| soc-delicious | 85498 | 85527.9 | - | 85488 | 85527.7 | 770.838 | 85503 | 85539.6 | - | 85686 | 85527.7 | - |
| soc-digg | 103238 | 103242.4 | 95.394 | 103240 | 103242.1 | - | 103240 | 103242.7 | - | 103244 | 103242.1 | - |
| soc-douban | 8685 | 8685 | 0.117 | 8685 | 8685 | 0.119 | 8685 | 8685 | 0.12 | 8685 | 8685 | 0.016 |
| soc-epinions | 9757 | 9757 | 0.163 | 9757 | 9757 | 0.161 | 9757 | 9757 | 0.097 | 9757 | 9757 | 0.298 |
| soc-flickr | 153271 | 153271.1 | 34.344 | 153271 | 153271.1 | 72.772 | 153271 | 153271 | 11.591 | 153272 | 153271.1 | - |
| soc-fixster | 96317 | 96317 | 6.404 | 96317 | 96317 | 5.856 | 96317 | 96317 | 4.035 | 96317 | 96317 | 4.596 |
| soc-FourSquare | 90108 | 90109.2 | 128.083 | 90108 | 90108.5 | 420.022 | 90108 | 90109.5 | 77.094 | 90109 | 90108.5 | - |
| soc-gowalla | 84222 | 84222.7 | 103.727 | 84222 | 84222.6 | 62.147 | 84222 | 84222.5 | 25.805 | 84222 | 84222.6 | 84.58 |
| soc-lastfm | 78688 | 78688 | 2.641 | 78688 | 78688 | 2.128 | 78688 | 78688 | 2.037 | 78688 | 78688 | 1.295 |
| soc-LiveMocha | 43427 | 43427 | 73.364 | 43427 | 43427 | 41.666 | 43427 | 43427 | 27.141 | 43427 | 43427 | 45.961 |
| soc-slashdot | 22373 | 22373 | 0.411 | 22373 | 22373 | 0.357 | 22373 | 22373 | 0.208 | 22373 | 22373 | 0.481 |
| soc-twitter-follows | 2323 | 2323 | 0.373 | 2323 | 2323 | 0.346 | 2323 | 2323 | 0.337 | 2323 | 2323 | 0.028 |
| soc-wiki-Vote | 406 | 406 | <0.001 | 406 | 406 | <0.001 | 406 | 406 | <0.001 | 406 | 406 | <0.001 |
| soc-youtube | 146376 | 146377 | 8.087 | 146376 | 146377 | 7.028 | 146376 | 146377 | 5.232 | 146376 | 146377 | 17.432 |
| soc-youtube-snap | 276945 | 276945.8 | 22.985 | 276945 | 276945 | 18.487 | 276945 | 276945.8 | 18.539 | 276945 | 276945.8 | 30.989 |
| power-US-Grid | 2203 | 2203 | 0.011 | 2203 | 2203 | 0.011 | 2203 | 2203 | 0.007 | 2203 | 2203 | 0.014 |
| USpowerGrid | 2203 | 2203 | 0.013 | 2203 | 2203 | 0.01 | 2203 | 2203 | 0.01 | 2203 | 2203 | 0.015 |
| 3elt | 3236 | 3236 | 287.811 | 3236 | 3236 | 3236.5 | 3236 | 3236 | 3236.8 | 436.833 | 3236 | 3236.5 |
| 3elt_dual | 4651 | 4651.7 | 544.364 | 4651 | 4652.3 | 555.858 | 4652 | 4653.4 | - | 4654 | 4652.3 | - |
| power | 2203 | 2203 | 0.011 | 2203 | 2203 | 0.01 | 2203 | 2203 | 0.011 | 2203 | 2203 | 0.014 |
| as-22july06 | 3303 | 3303 | 0.017 | 3303 | 3303 | 2.93 | 3303 | 3303 | 12.967 | 3303 | 3303 | 0.007 |
| chesapeake | 22 | 22 | <0.001 | 22 | 22 | <0.001 | 22 | 22 | <0.001 | 22 | 22 | <0.001 |
| polbooks | 62 | 62 | <0.001 | 62 | 62 | <0.001 | 62 | 62 | <0.001 | 62 | 62 | <0.001 |
| hamming8-2 | 254 | 254 | 0.001 | 254 | 254 | <0.001 | 254 | 254 | <0.001 | 254 | 254 | <0.001 |
| hamming8-4 | 240 | 240 | <0.001 | 240 | 240 | <0.001 | 240 | 240 | <0.001 | 240 | 240 | <0.001 |
| johnson32-2-4 | 465 | 465 | 0.017 | 465 | 465 | 0.016 | 465 | 465 | 0.01 | 465 | 465 | <0.001 |
| MANN-a45 | 1032 | 1032 | 0.085 | 1032 | 1032 | 0.084 | 1032 | 1032 | 0.085 | 1032 | 1032 | 0.015 |
| MANN-a81 | 3318 | 3318 | 0.871 | 3318 | 3318 | 0.877 | 3318 | 3318 | 1.11 | 3318 | 3318 | 0.183 |
| soc-dolphins | 34 | 34 | <0.001 | 34 | 34 | <0.001 | 34 | 34 | <0.001 | 34 | 34 | <0.001 |
| hamming10-2 | 1022 | 1022 | 0.07 | 1022 | 1022 | 0.071 | 1022 | 1022 | 0.08 | 1022 | 1022 | 0.01 |
| hamming10-4 | 1004 | 1004 | 0.056 | 1004 | 1004 | 0.053 | 1004 | 1004 | 0.061 | 1004 | 1004 | 0.011 |
| bio-celegans | 249 | 249 | <0.001 | 249 | 249 | <0.001 | 249 | 249 | <0.001 | 249 | 249 | <0.001 |
| bio-yeast | 456 | 456 | <0.001 | 456 | 456 | <0.001 | 456 | 456 | <0.001 | 456 | 456 | <0.001 |
| C1000-9 | 994 | 994 | 4.134 | 994 | 994 | 4.134 | 994 | 994 | 2.118 | 994 | 994 | 0.338 |
| C125-9 | 121 | 121 | <0.001 | 121 | 121 | <0.001 | 121 | 121 | 0.005 | 121 | 121 | <0.001 |
| C2000-5 | 1985 | 1985.1 | - | 1985 | 1985 | - | 1984 </td | | | | | |

Table 7: Experimental results on Network Repository (continued)

| | | | | | | | | | | | | |
|-------------------|---------------|-----------------|----------------|---------------|---------------|----------------|---------------|---------------|----------------|---------------|---------------|----------------|
| ca-coauthors-dblp | 472179 | 472179 | 35.184 | 472179 | 472179 | 23.723 | 472179 | 472179 | 12.502 | 472179 | 472179 | 33.352 |
| ca-CondMat | 12480 | 12480 | 0.063 | 12480 | 12480 | 0.053 | 12480 | 12480 | 0.039 | 12480 | 12480 | 0.044 |
| ca-dblp-2010 | 121969 | 121969 | 4.462 | 121969 | 121969 | 2.837 | 121969 | 121969 | 2.767 | 121969 | 121969 | 4.818 |
| ca-GrQc | 2208 | 2208 | 0.009 | 2208 | 2208 | 0.007 | 2208 | 2208 | 0.003 | 2208 | 2208 | 0.008 |
| CSphd | 550 | 550 | < 0.001 | 550 | 550 | < 0.001 | 550 | 550 | < 0.001 | 550 | 550 | < 0.001 |
| DSJC1000-5 | 985 | 985.6 | 104.475 | 985 | 985.1 | 203.892 | 985 | 985 | 61.892 | 985 | 985.1 | 3.973 |
| DSJC500-5 | 487 | 487 | 0.255 | 487 | 487 | 0.141 | 487 | 487 | 0.062 | 487 | 487 | 0.03 |
| email | 594 | 594 | 0.005 | 594 | 594 | 0.001 | 594 | 594 | 0.003 | 594 | 594 | < 0.001 |
| email-enron-large | 12781 | 12781 | 0.118 | 12781 | 12781 | 0.085 | 12781 | 12781 | 0.082 | 12781 | 12781 | 0.102 |
| email-enron-only | 86 | 86 | < 0.001 | 86 | 86 | < 0.001 | 86 | 86 | < 0.001 | 86 | 86 | < 0.001 |
| frb30-15-5 | 435 | 435 | 0.009 | 435 | 435 | 0.01 | 435 | 435 | 0.011 | 435 | 435 | < 0.001 |
| frb35-17-2 | 578 | 578 | 0.018 | 578 | 578 | 0.022 | 578 | 578 | 0.019 | 578 | 578 | 0.001 |
| frb35-17-3 | 578 | 578 | 0.018 | 578 | 578 | 0.018 | 578 | 578 | 0.018 | 578 | 578 | 0.003 |
| frb35-17-4 | 578 | 578 | 0.018 | 578 | 578 | 0.017 | 578 | 578 | 0.02 | 578 | 578 | 0.001 |
| frb35-17-5 | 578 | 578 | 0.021 | 578 | 578 | 0.02 | 578 | 578 | 0.02 | 578 | 578 | < 0.001 |
| frb40-19-1 | 741 | 741 | 0.031 | 741 | 741 | 0.035 | 741 | 741 | 0.032 | 741 | 741 | 0.003 |
| frb40-19-2 | 741 | 741 | 0.033 | 741 | 741 | 0.029 | 741 | 741 | 0.036 | 741 | 741 | 0.007 |
| frb40-19-3 | 741 | 741 | 0.034 | 741 | 741 | 0.031 | 741 | 741 | 0.032 | 741 | 741 | 0.006 |
| frb40-19-4 | 741 | 741 | 0.035 | 741 | 741 | 0.037 | 741 | 741 | 0.037 | 741 | 741 | 0.006 |
| frb40-19-5 | 741 | 741 | 0.035 | 741 | 741 | 0.035 | 741 | 741 | 0.033 | 741 | 741 | 0.003 |
| frb45-21-1 | 924 | 924 | 0.051 | 924 | 924 | 0.049 | 924 | 924 | 0.049 | 924 | 924 | 0.004 |
| frb45-21-2 | 924 | 924 | 0.05 | 924 | 924 | 0.049 | 924 | 924 | 0.047 | 924 | 924 | 0.002 |
| frb45-21-3 | 924 | 924 | 0.049 | 924 | 924 | 0.051 | 924 | 924 | 0.026 | 924 | 924 | 0.005 |
| frb45-21-4 | 924 | 924 | 0.052 | 924 | 924 | 0.053 | 924 | 924 | 0.03 | 924 | 924 | 0.002 |
| frb45-21-5 | 924 | 924 | 0.052 | 924 | 924 | 0.047 | 924 | 924 | 0.017 | 924 | 924 | 0.011 |
| frb50-23-1 | 1127 | 1127 | 0.074 | 1127 | 1127 | 0.067 | 1127 | 1127 | 0.09 | 1127 | 1127 | 0.016 |
| frb50-23-2 | 1127 | 1127 | 0.073 | 1127 | 1127 | 0.069 | 1127 | 1127 | 0.08 | 1127 | 1127 | 0.012 |
| frb50-23-3 | 1127 | 1127 | 0.074 | 1127 | 1127 | 0.067 | 1127 | 1127 | 0.083 | 1127 | 1127 | 0.014 |
| frb50-23-4 | 1127 | 1127 | 0.078 | 1127 | 1127 | 0.068 | 1127 | 1127 | 0.071 | 1127 | 1127 | 0.015 |
| frb50-23-5 | 1127 | 1127 | 0.069 | 1127 | 1127 | 0.071 | 1127 | 1127 | 0.086 | 1127 | 1127 | 0.012 |
| frb53-24-5 | 1248 | 1248 | 0.088 | 1248 | 1248 | 0.085 | 1248 | 1248 | 0.1 | 1248 | 1248 | 0.018 |
| frb59-26-1 | 1508 | 1508 | 0.128 | 1508 | 1508 | 0.128 | 1508 | 1508 | 0.138 | 1508 | 1508 | 0.024 |
| frb59-26-2 | 1508 | 1508 | 0.13 | 1508 | 1508 | 0.132 | 1508 | 1508 | 0.143 | 1508 | 1508 | 0.027 |
| frb59-26-3 | 1508 | 1508 | 0.128 | 1508 | 1508 | 0.133 | 1508 | 1508 | 0.141 | 1508 | 1508 | 0.024 |
| frb59-26-4 | 1508 | 1508 | 0.124 | 1508 | 1508 | 0.127 | 1508 | 1508 | 0.152 | 1508 | 1508 | 0.023 |
| frb59-26-5 | 1508 | 1508 | 0.13 | 1508 | 1508 | 0.126 | 1508 | 1508 | 0.134 | 1508 | 1508 | 0.028 |
| gen200-p0-9-44 | 195 | 195 | 0.005 | 195 | 195 | 0.005 | 195 | 195 | 0.004 | 195 | 195 | < 0.001 |
| gen200-p0-9-55 | 195 | 195 | 0.006 | 195 | 195 | 0.004 | 195 | 195 | 0.006 | 195 | 195 | 0.005 |
| gen400-p0-9-55 | 392 | 392.1 | 0.03 | 392 | 392.1 | 0.011 | 392 | 392.4 | 0.012 | 392 | 392.1 | 0.003 |
| gen400-p0-9-65 | 393 | 393 | 0.014 | 393 | 393 | 0.012 | 393 | 393.5 | 0.01 | 393 | 393 | 0.002 |
| gen400-p0-9-75 | 394 | 394 | 0.01 | 394 | 394 | 0.01 | 394 | 394 | 0.01 | 394 | 394 | 0.003 |
| ia-email-EU | 820 | 820 | 0.016 | 820 | 820 | 0.015 | 820 | 820 | 0.016 | 820 | 820 | < 0.001 |
| ia-email-univ | 594 | 594 | 0.002 | 594 | 594 | 0.002 | 594 | 594 | 0.003 | 594 | 594 | < 0.001 |
| ia-enron-large | 12781 | 12781 | 0.128 | 12781 | 12781 | 0.085 | 12781 | 12781 | 0.079 | 12781 | 12781 | 0.098 |
| ia-enron-only | 86 | 86 | < 0.001 | 86 | 86 | < 0.001 | 86 | 86 | < 0.001 | 86 | 86 | < 0.001 |
| ia-fb-messages | 578 | 578 | 0.008 | 578 | 578 | 0.007 | 578 | 578 | 0.005 | 578 | 578 | 0.001 |
| ia-infect-dublin | 293 | 293 | < 0.001 | 293 | 293 | < 0.001 | 293 | 293 | < 0.001 | 293 | 293 | 339.57 |
| keller5 | 745 | 745.2 | 0.032 | 745 | 745.2 | 0.033 | 745 | 745.2 | 0.04 | 745 | 745.2 | 0.009 |
| keller6 | 3298 | 3298 | 0.632 | 3298 | 3298 | 0.63 | 3298 | 3298 | 0.574 | 3298 | 3298 | 0.117 |
| pa2010 | 241120 | 241135.9 | 336.263 | 241192 | 241212 | - | 241189 | 241211.3 | - | 241236 | 241212 | - |
| minnesota | 1319 | 1319 | 0.011 | 1319 | 1319 | 0.006 | 1319 | 1319 | 0.001 | 1319 | 1319 | - |
| usroads | 65694 | 65699 | 701.152 | 65700 | 65704.2 | - | 65704 | 65708.9 | - | 65702 | 65704.2 | - |
| usroads-48 | 64206 | 64214.2 | 653.852 | 64214 | 64221.3 | - | 64219 | 64226.4 | - | 64221 | 64221.3 | - |

Table 8: Comparison of the initial solutions constructed by two methods: the GCNConstructVC and the GreedyConstructVC.

| Instance | GCNConstructVC | GreedyConstructVC | Instance | GCNConstructVC | GreedyConstructVC | Instance | GCNConstructVC | GreedyConstructVC |
|--------------|----------------|-------------------|------------|----------------|-------------------|--------------------------|----------------|-------------------|
| 144 | 121987 | 122465 | bio-yeast | 479 | 459(473) | ca-citeseer | 129330 | 129258 |
| 333SP | 2704261 | 2719254 | brock200-2 | 196 | 191(195) | ca-coauthors-dblp | 473913 | 472259 |
| 3elt | 3453 | 3480 | brock200-3 | 196 | 193(197) | ca-CondMat | 12509 | 12497 |
| 3elt_dual | 4896 | 4804 | brock200-4 | 196 | 192(194) | ca-dblp-2010 | 122108 | 122073 |
| 598a | 92792 | 92855 | brock400-1 | 395 | 394(394) | ca-GrQc | 2216 | 2214 |
| adaptive | 3408907 | 3408898 | brock400-4 | 396 | 395(396) | ca-HepPh | 6574 | 6565 |
| al2010 | 141044 | 143593 | brock800-1 | 793 | 794(794) | ca-MathSciNet | 140367 | 140446 |
| ar2010 | 104614 | 106477 | brock800-2 | 796 | (794) | ca2010 | 414221 | 422878 |
| as-22july06 | 3334 | 3325 | brock800-3 | 794 | 792(795) | caidaRouterLevel | 77323 | 78494 |
| AS365 | 2729194 | 2785283 | brock800-4 | 794 | 794(795) | channel-500x100x100-b050 | 3690904 | 3628053 |
| asia.osm | 6048471 | 6085708 | c-fat200-2 | 191 | 192(192) | citationCiteseer | 121242 | 123264 |
| auto | 377297 | 378817 | c-fat500-5 | 492 | 493(493) | co-papers-citeseer | 387314 | 386188 |
| az2010 | 134872 | 136926 | C250-9 | 248 | 246(248) | co2010 | 112754 | 114912 |
| belgium.osm | 733239 | 739448 | C4000-5 | 3993 | 3987(3991) | coAuthorsCiteseer | 129330 | 129258 |
| bio-celegans | 257 | 259 | ca-AstroPh | 11635 | 11521(11669) | coAuthorsDBLP | 155826 | 155756 |
| com AMAZON | 162253 | 163552 | G2 | 727 | 729 | inf-power | 2233 | 2271 |
| com DBLP | 165158 | 165084 | G22 | 1632 | 1649 | inf-road_central | 6926551 | 7165443 |
| coPapersDBLP | 473913 | 472259 | G23 | 1649 | 1654 | keller5 | 765 | 766 |
| cs4 | 14634 | 14749 | G24 | 1636 | 1646 | keller6 | 3348 | 3347 |
| CSPhd | 550 | 553 | G25 | 1643 | 1645 | ks2010 | 137881 | 141240 |
| ct2010 | 38569 | 39170 | G26 | 1652 | 1664 | ky2010 | 90537 | 92075 |
| cti | 9977 | 10046 | G3 | 726 | 733 | la2010 | 116350 | 119056 |
| data | 2237 | 2201 | G35 | 1336 | 1349 | loc-Brightkite | 22147 | 22146 |
| de2010 | 13789 | 14072 | G36 | 1343 | 1357 | loc-Gowalla | 85758 | 85538 |
| delaunay_n10 | 730 | 747 | G37 | 1344 | 1363 | luxembourg.osm | 57981 | 58239 |

Table 9: Comparison of the initial solutions constructed by two methods: the GCNConstructVC and the GreedyConstructVC.

| Instance | GCNConstructVC | GreedyConstructVC | Instance | GCNConstructVC | GreedyConstructVC | Instance | GCNConstructVC | GreedyConstructVC |
|--------------------|-----------------|-------------------|-----------------------|----------------|-------------------|----------------------------|----------------|-------------------|
| delaunay_n11 | 1449 | 1481 | G38 | 1325 | 1342 | m14b | 181813 | 182314 |
| delaunay_n12 | 2917 | 2963 | G43 | 824 | 832 | M6 | 2519414 | 2568592 |
| delaunay_n13 | 5811 | 5909 | G44 | 820 | 822 | ma2010 | 89588 | 91149 |
| delaunay_n14 | 11616 | 11831 | G45 | 824 | 831 | mc2010 | 78865 | 80115 |
| delaunay_n15 | 23165 | 23630 | G46 | 832 | 822 | mc2010 | 37619 | 38120 |
| delaunay_n16 | 46389 | 47258 | G47 | 811 | 821 | mn2010 | 190553 | 194920 |
| delaunay_n18 | 185812 | 189220 | G5 | 726 | 729 | minnesota | 1351 | 1392 |
| delaunay_n19 | 371735 | 378493 | G51 | 674 | 678 | mn2010 | 147466 | 150786 |
| delaunay_n20 | 743387 | 757013 | G52 | 674 | 687 | mo2010 | 191364 | 194923 |
| delaunay_n21 | 1486424 | 1513884 | G53 | 677 | 683 | ms2010 | 96601 | 98326 |
| delaunay_n22 | 2972220 | 3028303 | G54 | 681 | 684 | mt2010 | 72256 | 73462 |
| delaunay_n23 | 5944908 | 6057125 | G58 | 3342 | 3367 | mycileskian10 | 405 | 403 |
| DSJC500-5 | 491 | 490 | G63 | 4675 | 4711 | mycileskian11 | 806 | 807 |
| email | 613 | 615 | ga2010 | 164588 | 167349 | mycileskian12 | 1605 | 1600 |
| email-enron-large | 12854 | 12822 | gen200-p0-9-44 | 196 | 197 | mycileskian13 | 3215 | 3217 |
| email-enron-only | 88 | 87 | gen400-p0-9-75 | 397 | 395 | mycileskian14 | 6378 | 6370 |
| fe-4el2 | 8052 | 8119 | germany.osm | 5830163 | 5892463 | mycileskian15 | 12815 | 12807 |
| fe-ocean | 82889 | 80426 | great-britain.osm | 3853211 | 3890029 | mycileskian16 | 25413 | 25398 |
| fe-sphere | 11784 | 11016 | hi2010 | 14276 | 14531 | mycileskian17 | 51085 | 51027 |
| fe-tooth | 50660 | 50753 | hugetrace-00000 | 2677698 | 2677603 | mycileskian9 | 201 | 202 |
| fe_rotor | 81902 | 82132 | hugetrace-00010 | 7000430 | 6990029 | nc2010 | 162720 | 165661 |
| f2010 | 273900 | 279242 | hugetrace-00020 | 9438065 | 9418528 | nd2010 | 75236 | 76695 |
| frb30-15-5 | 442 | 443 | hugetrinsic-00000 | 3938525 | 3928096 | ne2010 | 110934 | 113339 |
| frb35-17-2 | 578 | 587 | hugetrinsic-00010 | 4248609 | 4237685 | netherlands.osm | 1130535 | 1149044 |
| frb35-17-5 | 587 | 589 | hugetrinsic-00020 | 5938525 | 5938525 | nh2010 | 26347 | 26694 |
| frb40-19-1 | 741 | 745 | ia-email-EU | 828 | 827 | nj2010 | 99449 | 101564 |
| frb40-19-2 | 741 | 753 | ia-email-univ | 613 | 615 | NLR | 2994993 | 3053479 |
| frb40-19-3 | 741 | 751 | ia-enron-large | 12854 | 12822 | nm2010 | 93635 | 95170 |
| frb40-19-4 | 747 | 753 | ia-enron-only | 88 | 87 | nv2010 | 47107 | 47842 |
| frb40-19-5 | 741 | 752 | ia-fb-messages | 589 | 592 | oh2010 | 209972 | 214215 |
| frb45-21-1 | 938 | 924 | ia-infect-dublin | 299 | 300 | ok2010 | 151311 | 154481 |
| frb45-21-2 | 935 | 939 | ia-wiki-Talk | 17448 | 17464 | or2010 | 109813 | 111561 |
| frb45-21-3 | 938 | 924 | ia2010 | 126447 | 129524 | p-hat1000-1 | 937 | 938 |
| frb50-23-1 | 1127 | 1141 | id2010 | 80701 | 81836 | p-hat1000-2 | 952 | 953 |
| frb50-23-4 | 1138 | 1139 | il2010 | 268529 | 275355 | p-hat1500-1 | 1423 | 1424 |
| frb53-24-5 | 1262 | 1248 | in2010 | 155328 | 158853 | p-hat1500-2 | 1449 | 1450 |
| frb59-26-3 | 1529 | 1508 | inf-asia.osm | 6048471 | 6085708 | p-hat1500-3 | 1492 | 1491 |
| frb59-26-5 | 1508 | 1523 | inf-belgium.osm | 732329 | 739448 | p-hat500-2 | 469 | 468 |
| G1 | 727 | 726 | inf-germany.osm | 5830163 | 5892463 | p-hat700-1 | 643 | 644 |
| G14 | 540 | 548 | inf-great-britain.osm | 3853211 | 3890029 | p-hat700-3 | 692 | 693 |
| G15 | 535 | 540 | inf-italy.osm | 3390659 | 3399601 | pa2010 | 246941 | 252018 |
| G16 | 530 | 533 | inf-luxembourg.osm | 57981 | 58239 | polbooks | 63 | 65 |
| G17 | 530 | 537 | inf-netherlands.osm | 1130535 | 1149044 | power | 2233 | 2271 |
| power-US-Grid | 2233 | 2271 | soc-brightkite | 21470 | 21469 | tn2010 | 136762 | 142226 |
| prefrentAttachment | 60908 | 61680 | soc-buzznet | 31828 | 31795 | tx2010 | 526576 | 550104 |
| ri2010 | 14713 | 14957 | soc-delicious | 88268 | 90812 | uk | 2824 | 2816 |
| road_centeral | 6926551 | 7165443 | soc-digg | 107009 | 106831 | USpowerGrid | 2233 | 2350 |
| road_usa | 11811200 | 12200485 | soc-douban | 8693 | 8704 | usroads | 65865 | 70088 |
| san1000 | 935 | 933 | soc-opinions | 9853 | 9860 | usroads-48 | 67362 | 68511 |
| san200-0-9-3 | 195 | 197 | soc-flickr | 154595 | 154471 | ut2010 | 63273 | 65714 |
| san400-0-5-1 | 377 | 369 | soc-flixster | 96804 | 96873 | va2010 | 157038 | 162934 |
| san400-0-7-1 | 392 | 390 | soc-FourSquare | 91041 | 90719 | venturiLevel3 | 2031366 | 2030900 |
| san400-0-7-2 | 394 | 390 | soc-gowalla | 85758 | 85558 | vsp_sctapl-2b_and_seymourl | 18431 | 18939 |
| san400-0-7-3 | 381 | 385 | soc-lastfm | 80184 | 80205 | vt2010 | 17725 | 18351 |
| san200-0-9 | 197 | 196 | soc-LiveMocha | 44922 | 45314 | wa2010 | 111427 | 116261 |
| sc2010 | 102693 | 104406 | soc-slashdot | 22688 | 22665 | wi2010 | 144973 | 151667 |
| scc_infect-dublin | 9132 | 9124 | soc-twitter-follows | 2376 | 2419 | wing | 40570 | 40999 |
| scc_infect-hyper | 110 | 110 | soc-wiki-Vote | 415 | 414 | wing_nodal | 9159 | 9409 |
| scc_reality | 2490 | 2486 | soc-youtube | 279661 | 149089 | wv2010 | 72389 | 75019 |
| sd2010 | 50722 | 52052 | soc-youtube-snap | 149198 | 279389 | soc-BlogCatalog | 21281 | 21257 |
| smallworld | 78261 | 79350 | t60k | 30667 | 30533 | | | |

Table 10: Comparison of solution quality between No_CRV and GCNIVC.

| Instance | No_CRV | GCNIVC | Instance | No_CRV | GCNIVC | Instance | No_CRV | GCNIVC |
|-------------------|----------------|----------------|-----------------------|---------|----------------|----------------------------|----------|-----------------|
| 144 | 117819 | 117820 | ia2010 | 123121 | 123075 | NLR | 2882055 | 2881932 |
| 333SP | 2545721 | 2546845 | id2010 | 79175 | 79173 | nm2010 | 91779 | 91765 |
| 598a | 89162 | 89164 | il2010 | 261156 | 261001 | nv2010 | 46165 | 46157 |
| al2010 | 138528 | 138512 | in2010 | 151508 | 151460 | oh2010 | 205511 | 205441 |
| ar2010 | 102554 | 102547 | inf-asia.osm | 5965693 | 5965475 | ok2010 | 147627 | 147566 |
| AS365 | 2629649 | 2629682 | inf-belgium.osm | 716873 | 716867 | or2010 | 107643 | 107622 |
| asia.osm | 5963763 | 5965052 | inf-germany.osm | 5778444 | 5741704 | pa2010 | 241211 | 241120 |
| auto | 364598 | 364594 | inf-great-britain.osm | 3794838 | 3775859 | road_central | 6924682 | 6855046 |
| az2010 | 132203 | 132183 | inf-italy.osm | 3334878 | 3334068 | road_usa | 11844139 | 11772344 |
| belgium.osm | 716870 | 716868 | inf-netherlands.osm | 1100078 | 1100046 | sc2010 | 100847 | 100844 |
| ca2010 | 404321 | 404197 | inf-road_central | 6886386 | 6856610 | smallworld | 75546 | 75541 |
| caidaRouterLevel | 75197 | 75193 | ks2010 | 134377 | 134310 | soc-delicious | 85501 | 85498 |
| citationCiteseer | 118143 | 118133 | ky2010 | 88791 | 88783 | soc-digg | 103241 | 103238 |
| co2010 | 110118 | 110073 | la2010 | 113471 | 113448 | 160k | 30332 | 30324 |
| com-Amazon | 160240 | 160242 | m14b | 175785 | 175773 | tn2010 | 134350 | 134349 |
| cs4 | 13339 | 13345 | M6 | 2423910 | 2423393 | tx2010 | 513090 | 512894 |
| ct2010 | 37959 | 37958 | ma2010 | 87950 | 87947 | usroads | 65699 | 65694 |
| delaunay_n14 | 11229 | 11228 | md2010 | 77496 | 77495 | usroads-48 | 64213 | 64206 |
| delaunay_n18 | 179581 | 179579 | me2010 | 37053 | 37052 | ut2010 | 62146 | 62142 |
| delaunay_n19 | 359127 | 359123 | mi2010 | 185892 | 185819 | va2010 | 154264 | 154257 |
| delaunay_n20 | 718290 | 718224 | mn2010 | 144064 | 144013 | venturiLevel3 | 2026333 | 2026295 |
| delaunay_n21 | 1436537 | 1436518 | mo2010 | 187702 | 187679 | vsp_sctap1-2b_and_seymourl | 17785 | 17784 |
| delaunay_n22 | 2873160 | 2873088 | ms2010 | 94944 | 94936 | wa2010 | 108821 | 108793 |
| delaunay_n23 | 5851454 | 5831454 | mt2010 | 70644 | 70631 | wi2010 | 141709 | 141664 |
| fe-ocean | 72086 | 72173 | nc2010 | 159854 | 159831 | wing | 36888 | 36879 |
| fl2010 | 267019 | 266945 | nd2010 | 73700 | 73681 | wv2010 | 71169 | 71166 |
| ga2010 | 161701 | 161677 | ne2010 | 108224 | 108184 | wy2010 | 46756 | 46748 |
| germany.osm | 5707867 | 5707860 | netherlands.osm | 1100078 | 1100047 | | | |
| great-britain.osm | 3775520 | 3775495 | nj2010 | 96819 | 96795 | | | |

Table 11: Comparison of solution quality between No_Dcnumber and GCNIVC.

| Instance | No_Dcnumber | GCNIVC | Instance | No_Dcnumber | GCNIVC | Instance | No_Dcnumber | GCNIVC |
|--------------------------|---------------|----------------|-----------------------|---------------|----------------|----------------------------|--------------|-----------------|
| 144 | 117802 | 117820 | ia2010 | 123119 | 123075 | nm2010 | 91779 | 91765 |
| 333SP | 2565721 | 2546845 | id2010 | 79182 | 79173 | nv2010 | 46165 | 46157 |
| 598a | 89174 | 89164 | il2010 | 261156 | 261001 | oh2010 | 205498 | 205441 |
| al2010 | 138520 | 138512 | in2010 | 151494 | 151460 | ok2010 | 147618 | 147566 |
| ar2010 | 102551 | 102547 | inf-asia.osm | 6010304 | 5965475 | or2010 | 107636 | 107622 |
| AS365 | 2630248 | 2629682 | inf-belgium.osm | 716870 | 716867 | pa2010 | 241191 | 241120 |
| asia.osm | 5992845 | 5965052 | inf-germany.osm | 5786664 | 5741704 | road_central | 6966221 | 6855046 |
| auto | 364599 | 364594 | inf-great-britain.osm | 3794838 | 3775859 | road_usa | 11833068 | 11772344 |
| az2010 | 132205 | 132183 | inf-italy.osm | 3334648 | 3334068 | se2010 | 100849 | 100844 |
| belgium.osm | 716878 | 716868 | inf-netherlands.osm | 1100078 | 1100046 | smallworld | 75546 | 75541 |
| ca2010 | 404322 | 404197 | inf-road_central | 6888692 | 6856610 | soc-delicious | 85505 | 85498 |
| caidaRouterLevel | 75200 | 75193 | ks2010 | 134379 | 134310 | soc-digg | 103240 | 103238 |
| channel-500x100x100-b050 | 3608700 | 3601693 | ky2010 | 88785 | 88783 | t60k | 30332 | 30324 |
| citationCiteseer | 118138 | 118133 | la2010 | 113479 | 113448 | tn2010 | 134358 | 134349 |
| co2010 | 110114 | 110073 | m14b | 175772 | 175773 | tx2010 | 513106 | 512894 |
| cs4 | 13347 | 13345 | M6 | 2427627 | 2423393 | usroads | 65689 | 65694 |
| ct2010 | 37959 | 37958 | ma2010 | 87948 | 87947 | usroads-48 | 64210 | 64206 |
| delaunay_n18 | 179584 | 179579 | me2010 | 37053 | 37052 | ut2010 | 62151 | 62142 |
| delaunay_n20 | 718258 | 718224 | mi2010 | 185889 | 185819 | va2010 | 154259 | 154257 |
| delaunay_n21 | 1436537 | 1436518 | mn2010 | 144051 | 144013 | venturiLevel3 | 2026320 | 2026295 |
| delaunay_n22 | 2873160 | 2873088 | mo2010 | 187694 | 187679 | vsp_sctap1-2b_and_seymourl | 17785 | 17784 |
| delaunay_n23 | 5892351 | 5831454 | ms2010 | 94943 | 94936 | wa2010 | 108822 | 108793 |
| fe-4elt2 | 7574 | 7572 | mt2010 | 70635 | 70631 | wi2010 | 141701 | 141664 |
| fe_ocean | 72341 | 72173 | nc2010 | 159854 | 159831 | wing | 36837 | 36879 |
| fe_rotor | 77611 | 77615 | nd2010 | 73699 | 73681 | wv2010 | 71181 | 71166 |
| fl2010 | 267017 | 266945 | ne2010 | 108208 | 108184 | wy2010 | 46751 | 46748 |
| ga2010 | 161700 | 161677 | netherlands.osm | 1100064 | 1100047 | venturiLevel3 | 2026333 | 2026295 |
| germany.osm | 5707867 | 5707860 | nj2010 | 96811 | 96795 | sd2010 | 49303 | 49302 |
| great-britain.osm | 3775520 | 3775495 | NLR | 2884302 | 2881932 | | | |